

---

# Optimal Observation-Intervention Trade-Off in Optimisation Problems with Causal Structure

---

Kim Hammar<sup>†</sup>

KTH Royal Institute of Technology  
Stockholm, Sweden  
kimham@kth.se

Neil Dhir<sup>†</sup>

Siemens Technology  
Berkeley, California, USA  
neil.dhir@siemens.com

## Abstract

We consider the problem of optimising an expensive-to-evaluate grey-box objective function, within a finite budget, where known side-information exists in the form of the causal structure between the design variables. Standard black-box optimisation ignores the causal structure, often making it inefficient and expensive. The few existing methods that consider the causal structure are myopic and do not fully accommodate the observation-intervention trade-off that emerges when estimating causal effects. In this paper, we show that the observation-intervention trade-off can be formulated as a non-myopic optimal stopping problem which permits an efficient solution. We give theoretical results detailing the structure of the optimal stopping times and demonstrate the generality of our approach by showing that it can be integrated with existing causal Bayesian optimisation algorithms. Experimental results show that our formulation can enhance existing algorithms on real and synthetic benchmarks.

## 1 Introduction

This paper studies global optimisation of an expensive-to-evaluate *grey-box* [5] objective function with known causal structure in the form of a *causal diagram* (making it grey-box rather than ‘black-box’). In this setting, inputs to the objective function correspond to *interventions* and outputs correspond to causal effects. We assume that the objective function can be evaluated (possibly with noise) at a finite number of inputs, either by measurement or some estimation procedure. Each evaluation is associated with a cost and a finite budget of total evaluations is prescribed. Since no known functional form of the objective function is available, our goal is to find an input that optimises the objective function by estimating the causal effects of a sequence of interventions. This estimation can be done in two ways: *i*) by intervening and conducting controlled experiments; and *ii*) by passively observing and using the causal graph to estimate the causal effects (*vis-à-vis* the do-calculus [45]). In choosing between these two options, an *observation-intervention* trade-off emerges. On the one hand, interventions are costly but allow us to reliably estimate causal effects. On the other hand, observations are (usually) cheap to collect but may not always be sufficient to identify causal effects. We show that this trade-off can be formulated as an *optimal stopping* problem that permits an efficient solution [66, 54, 16].

Two principal algorithmic frameworks have been developed to solve optimisation problems of the type described above: *i*) causal Bayesian optimisation (CBO) algorithms [2, 3, 60, 15], which assume that the objective function is defined over a continuous domain; and *ii*) causal multi-armed bandit (MAB) algorithms [31, 9, 37, 29, 35], which assume that the objective function is defined over a discrete set of inputs. To our knowledge, no hybrid approach exists. Compared to standard Bayesian optimisation (BO) and MABs, which ignore the causal structure of the problem, CBO and causal MABs

---

<sup>†</sup>Equal contribution.

are able to exploit the causal structure to improve sample efficiency. A drawback of the existing causal approaches, however, is that they are *myopic* in the sense that they do not consider more than one step into the future when deciding on interventions. Another limitation is that the existing approaches rely on heuristics to balance the observation-intervention trade-off and do not quantify the cost of observing. Specifically, in the CBO setting, an  $\epsilon$ -greedy strategy is adopted by Aglietti et al. [2] and a myopic exploration approach is adopted by Sussex et al. [60] and the trade-off is ignored in [3, 15]. In the causal MAB setting, a heuristic approach is used by Lattimore et al. [31] and the work in [9, 37, 29, 35] uses myopic exploration approaches similar to Sussex et al. [60]. Moreover, all of the approaches referenced above assume a) that an arbitrary number of observations can be collected; and b) that there are no costs associated with collecting observations. These assumptions are not realistic in many scenarios: to test for high cholesterol in the US, a blood-test (observation) is required which costs on average \$51 [21] and the requisite intervention (statins) costs \$139 [27]. Similarly, a prostate-specific antigen test to screen for prostate cancer (observation) costs on average \$40 [1] and the cost of a radical prostatectomy procedure (intervention) is on average \$34,720 [43, 26].

**Main contributions.** Motivated by the above shortcomings in existing work, we present a general approach to extend existing CBO algorithms (the results are fully extendable to the causal MAB setting) to balance the intervention-observation trade-off in an optimal and *non-myopic* way, while taking observation costs into account. From hereon, for brevity, we refer to our approach as *Optimal Stopping for Causal Optimisation* (OSCO). Our main contributions are:

- We formulate the observation-intervention trade-off as an *optimal stopping* problem whose solution determines whether a given intervention should be carried out or if it is more cost-effective to collect observational data.
- We prove that the solution to the optimal stopping problem can be computed efficiently and show that it can enhance existing CBO (and causal MAB) algorithms.
- We characterise a set of variables called the *minimal observation set* (MOS), which is the minimal set of variables that need to be observed to estimate the causal effect of an intervention.

## 2 Theoretical background

This section covers notations and theoretical background on structural causal models. The models and definitions introduced here provide a foundation for the subsequent section where we describe our problem statement. A table of notations is available in Appendix A. Finally, to ensure that the narrative remains fluid we also introduce the MOS in this section.

### 2.1 Structural causal models

**Structural causal models.** A Structural Causal Model (SCM) [45, Ch. 7, Def 7.1.1] is a semantic framework to model the causal mechanisms of a system. Let  $\mathcal{M}$  be a SCM parametrised by the quadruple  $\langle \mathbf{U}, \mathbf{V}, \mathbf{F}, P(\mathbf{U}) \rangle$ . Here  $\mathbf{U}$  is a set of exogenous variables which follow a joint distribution  $P(\mathbf{U})$  and  $\mathbf{V}$  is a set of endogenous (observed) variables. Within  $\mathbf{V}$  we distinguish between three types of variables: manipulative  $\mathbf{X} \subseteq \mathbf{V} \setminus \mathbf{Y} \setminus \mathbf{N}$ ; non-manipulative  $\mathbf{N} \subseteq \mathbf{V} \setminus \mathbf{X}$  and targets (outcome variables)  $\mathbf{Y} \subseteq \mathbf{N}$ .

Graphically, each SCM induces a causal diagram (a directed acyclic graph, DAG for short)  $\mathcal{G} = \langle \mathbf{V}, \mathbf{E} \rangle$ . Each vertex in the graph corresponds to a variable and the directed arcs point from members of  $\text{pa}(V_i)_{\mathcal{G}}$  and  $U_i$  toward  $V_i$ , where  $\text{pa}(V_i)_{\mathcal{G}}$  denotes the parent nodes of  $V_i$  in  $\mathcal{G}$  [45, Ch. 7]. The arcs represent a set of functions  $\mathbf{F} \triangleq \{f_i\}_{V_i \in \mathbf{V}}$  [36, §1]. Each function  $f_i$  is a mapping from (the respective domains of  $U_i \cup \text{pa}(V_i)_{\mathcal{G}}$  to  $V_i$  – where  $U_i \subseteq \mathbf{U}$  and  $\text{pa}(V_i)_{\mathcal{G}} \subseteq \mathbf{V} \setminus V_i$ . A bidirected arc between  $V_i$  and  $V_j$  occurs if they share an unobserved confounder, i.e. if  $\mathbf{U}_i \cap \mathbf{U}_j \neq \emptyset$  [34]. If each function  $f_i \in \mathbf{F}$  is independent of time, the SCM is said to be stationary and if both  $\mathbf{U}$  and  $\mathbf{V}$  are finite the SCM is said to be finite. For a more incisive discussion on the properties of SCMs we refer the reader to [45, 7].

**Causal effects of interventions.** The do-operator  $\text{do}(\mathbf{X} = \mathbf{x})$  represents the causal effect of an intervention that fixes a set of endogenous variable(s)  $\mathbf{X}$  to constant value(s)  $\mathbf{x}$  irrespective of their original mechanisms  $\mathbf{F}$ . This operation can be represented graphically by removing the incoming

arcs to  $\mathbf{X}$  in  $\mathcal{G}$ . We denote by  $\mathcal{G}_{\overline{\mathbf{X}}}$  the mutilated graph obtained by deleting from  $\mathcal{G}$  all arcs pointing to nodes in  $\mathbf{X}$ . Examples of mutilated graphs are shown in Fig. 1.

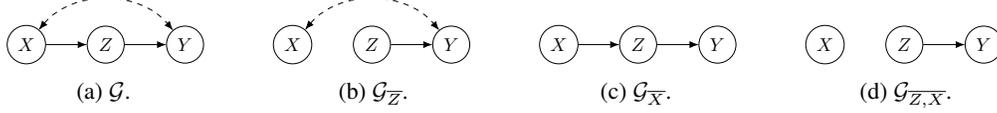


Figure 1: Mutilated causal diagrams; nodes represent variables in an SCM; solid edges represent causal relations and dashed edges represent unobserved confounding; the diagrams represent post-intervention worlds where a specific intervention has been implemented, from left to right, these are:  $\text{do}(\emptyset)$ ,  $\text{do}(Z)$ ,  $\text{do}(X)$  and  $\text{do}(X, Z)$ ; interventions are graphically represented with the incoming arcs onto the intervention removed.

**Estimating causal effects.** The goal of causal inference is to generate probabilistic formulas for the effects of interventions in terms of observation probabilities. In this work we accomplish this by employing Pearl [45]’s do-calculus, which is an axiomatic system for replacing probability formulas containing the do-operator with ordinary conditional probabilities. Application of the do-calculus requires the interventions to be uniquely determined from  $P(\mathbf{V})$  and  $\mathcal{G}$ . Determining if this is the case is known as the *problem of identification* and has received considerable attention in the causal inference literature [46, 45, 56, 57, 63, 62], formally:

**Definition 1.** Causal effect identifiability [6, Def. 1]. Let  $\mathbf{X}, \mathbf{Y}$  be two sets of disjoint variables and let  $\mathcal{G}$  be the causal diagram. The causal effect of an intervention  $\text{do}(\mathbf{X} = \mathbf{x})$  on a set of variables  $\mathbf{Y}$  is said to be identifiable from  $P$  in  $\mathcal{G}$  if  $P(\mathbf{Y} \mid \text{do}(\mathbf{X} = \mathbf{x}))$  is *uniquely* computable from  $P(\mathbf{V})$  in any causal model that induces  $\mathcal{G}$ .

## 2.2 Sets of endogenous variables

**Intervention sets.** Given a causal graph  $\mathcal{G}$  of an SCM  $\mathcal{M} \triangleq \langle \mathbf{U}, \mathbf{V}, \mathbf{F}, P(\mathbf{U}) \rangle$  with a set of manipulative variables  $\mathbf{X}$  and a target variable  $Y$ , we can define *minimal intervention sets*, which represent non-redundant intervention sets for achieving an effect on  $Y$ :

**Definition 2.** Minimal intervention set (MIS) [35, Def. 2]. A set of manipulative variables  $\mathbf{X} \subseteq \mathbf{V} \setminus \{Y\} \setminus \mathbf{N}$  is said to be a MIS for  $Y$  if there is no  $\mathbf{X}' \subset \mathbf{X}$  such that  $\mathbb{E}[Y \mid \text{do}(\mathbf{X} = \mathbf{x})] = \mathbb{E}[Y \mid \text{do}(\mathbf{X}' = \mathbf{x}')] \text{ for every SCM induced by } \mathcal{G}$ . Denote by  $\mathbf{M}_{\mathcal{G}, Y}^{\mathbf{V}}$  a set of MISs given the SCM  $\mathcal{M}$ .

A subset of the set of MISs can lead to the minimal value of  $Y$ :

**Definition 3.** Possibly optimal minimal intervention set (POMIS) [35, Def. 3].  $\mathbf{X} \in \mathbf{M}_{\mathcal{G}, Y}^{\mathbf{V}}$  is a POMIS if there exists an SCM induced by  $\mathcal{G}$  such that  $\mathbb{E}[Y \mid \text{do}(\mathbf{X} = \mathbf{x}^*)] < \mathbb{E}[Y \mid \text{do}(\mathbf{W} = \mathbf{w}^*)] \forall \mathbf{W} \in \mathbf{M}_{\mathcal{G}, Y}^{\mathbf{V}} \setminus \mathbf{X}$ . Denote by  $\mathbf{P}_{\mathcal{G}, Y}^{\mathbf{V}}$  a set of POMISs given the SCM  $\mathcal{M}$ .

**Observation sets.** The solution to the *identification problem* [57] tells us under what conditions the effect of a given intervention can be computed from  $P(\mathbf{V})$  and the causal diagram  $\mathcal{G}$ . A number of sound and complete algorithms exist which solve this problem [55, 57, 61, 25]. The solution, if it exists as per Def. 1, returns an expression  $Q_Y^{\mathbf{X}}$  which only contains observational measures. The set of variables  $\mathbf{Z} \subseteq \mathbf{V}$  occurring in  $Q_Y^{\mathbf{X}}$  is the *minimal observation set*, which we introduce and formally define as

**Definition 4.** Minimal observation set (MOS). If  $P(Y \mid \text{do}(\mathbf{X} = \mathbf{x}))$  is identifiable as per Def. 1 then  $\exists Q_Y^{\mathbf{X}}$ . If a)  $Q_Y^{\mathbf{X}}$  can be estimated by observing  $\mathbf{Z} \subseteq \mathbf{V}$  and b)  $\nexists \mathbf{Z}' \subset \mathbf{Z}$  that allows us to estimate  $Q_Y^{\mathbf{X}}$ , then  $\mathbf{Z}$  is a MOS. The MOS which follows  $Q_Y^{\mathbf{X}}$  is denoted by  $\mathbf{O}_{\mathcal{G}, Y}^{\mathbf{X}}$ .

We demonstrate Def. 4 by considering the causal diagrams in Fig. 2. Applying the rules of do-calculus we can express the interventional distributions in terms of observational mass functions:

$$P(Y \mid \text{do}(B = b)) = \sum_S P(Y \mid B, S) P(S) = Q_Y^{\{B\}} \quad (1)$$

$$P(Y \mid \text{do}(B = b), \text{do}(W = w)) = \sum_S P(Y \mid B, W, S) P(S) = Q_Y^{\{B, W\}} \quad (2)$$

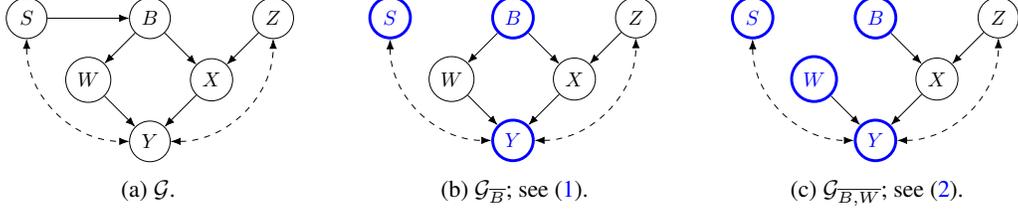


Figure 2: Causal diagram  $\mathcal{G}$  shown in Fig. 2a with two post-intervention worlds in Fig. 2b and Fig. 2c. Blue node colour indicates the minimal set of variables which need to be measured to estimate the identifiable causal effect.

The MOS relative to  $Q_Y^{\{B\}}$ , shown on the right-hand-side (RHS) in (1) is  $\mathbf{O}_{\mathcal{G},Y}^{\{B\}} = \{Y, B, S\}$  with the mutilated causal diagram shown in Fig. 2b. Similarly for Fig. 2c the MOS is given by  $\mathbf{O}_{\mathcal{G},Y}^{\{B,W\}} = \{Y, B, W, S\}$ , with  $Q_Y^{\{B,W\}}$  given on the RHS in (2).

### 3 Problem statement

Consider a causal graph  $\mathcal{G}$  that encodes the causal relationship among a finite set of variables  $\mathbf{V}$  in a stationary SCM  $\mathcal{M} = \langle \mathbf{U}, \mathbf{V}, \mathbf{F}, P(\mathbf{U}) \rangle$ . We are interested in manipulating  $\mathbf{X} \subseteq \mathbf{V}$  to minimise a target variable  $Y \in \mathbf{V} \setminus \mathbf{X}$ , which we assume is bounded, i.e.  $|y| \leq M < \infty$  for some  $M \in \mathbb{R}$  and all  $y \in \text{dom}(Y)$ . This objective is formally expressed as

$$\begin{aligned} & \underset{\substack{\mathbf{X}' \in \mathbf{P}_{\mathcal{G},Y}^{\mathbf{V}}; \\ \mathbf{x}' \in \text{dom}(\mathbf{X}')}}}{\text{minimise}} \mu(\mathbf{X}', \mathbf{x}') \triangleq \mathbb{E}[Y \mid \text{do}(\mathbf{X}' = \mathbf{x}')] \end{aligned} \quad (3)$$

We assume that interventions are atomic (also known as ‘hard’ [60] or ‘perfect’) as modelled by the do-operator [45]. ‘Soft’ or ‘stochastic’ [17] intervention settings are left for future work. We further assume that the functional relationships in  $\mathcal{M}$  (i.e.  $\mathbf{F}$ ) are unknown (but  $\mathcal{G}$  is assumed known), which means that minimising (3) requires estimating  $\mathbb{E}[Y \mid \text{do}(\mathbf{X}' = \mathbf{x}')] from data. This estimation can be done in two ways: *i*) by intervening and conducting a controlled experiment, which yields samples from the interventional distribution  $P(Y \mid \text{do}(\mathbf{X}' = \mathbf{x}'))$ ; and *ii*) by passively observing  $\mathbf{O}_{\mathcal{G},Y}^{\mathbf{X}'}$  (see Def. 4) and using  $\mathcal{G}$  to estimate the causal effect through the do-calculus [44] (given that the causal effect is identifiable, otherwise the causal effect has to be estimated by intervening). Both estimation procedures are perturbed by additive Gaussian noise  $\epsilon_t \sim \mathcal{N}(0, \sigma^2)$  and involve costs. Denote with  $c(\mathbf{X}', e_t = \mathfrak{I})$  the cost of estimating  $\mathbb{E}[Y \mid \text{do}(\mathbf{X}' = \mathbf{x}')] by intervening and denote with  $c(\mathbf{X}', e_t = \mathfrak{O})$  the cost of estimating the same expression by observing. The problem, then, is to design a sequence of interventions  $(\text{do}(\mathbf{X}'_t = \mathbf{x}'_t))_{t \in \{1, \dots, T\}}$  and a sequence of estimation procedures  $(e_t)_{t \in \{1, \dots, T\}}$  to find an intervention that minimises (3) while keeping the cumulative cost below a maximum cost  $K$ . This problem can be formally stated as$$

$$\underset{\substack{t, \mathbf{X}'_t, \mathbf{x}'_t \\ t \in \{1, \dots, T\}}}{\text{minimise}} \left\{ \min_{t \in \{1, \dots, T\}} \mu(\mathbf{X}'_t, \mathbf{x}'_t) - \mu(\mathbf{X}^*, \mathbf{x}^*) \right\} \quad (4a)$$

$$\text{subject to} \quad \sum_{t=1}^T c(\mathbf{X}'_t, e_t) < K, \quad \mathbf{X}'_t \in \mathbf{P}_{\mathcal{G},Y}^{\mathbf{V}}, \quad \mathbf{x}'_t \in \text{dom}(\mathbf{X}'_t) \quad \forall t \in \{1, \dots, T\} \quad (4b)$$

$$e_t \in \begin{cases} \{\mathfrak{I}, \mathfrak{O}\} & \text{if } P(Y \mid \text{do}(\mathbf{X}'_t = \mathbf{x}'_t)) \text{ is identifiable} \\ \{\mathfrak{I}\} & \text{otherwise} \end{cases} \quad \forall t \in \{1, \dots, T\} \quad (4c)$$

where  $(\mathbf{X}^*, \mathbf{x}^*)$  denotes the minimiser of (3) and the expression inside the brackets of (4a) is the simple regret metric [22]. Further, (4b) – (4c) define the cost and domain constraints. The time-horizon  $T$  is defined as the largest  $t \in \mathbb{N}$  for which (4b) is satisfied.

The above problem is challenging for two reasons. First, to select the optimal intervention  $\text{do}(\mathbf{X}'_t = \mathbf{x}'_t)$  to evaluate at each stage  $t \in \{1, \dots, T\}$ , it is necessary to take into account both *exploration* (evaluating the causal effects in regions of high uncertainty) and *exploitation* (evaluating

the causal effects in regions deemed promising based on previous evaluations). Second, in selecting the evaluation procedures  $(e_t)_{t \in \{1, \dots, T\}}$ , it is necessary to balance the trade-off between *intervening* (estimating causal effects through controlled experimental evaluations) and *observing* (estimating causal effects through the do-calculus).

The exploration-exploitation trade-off is well-studied in the statistical learning literature (see textbooks [22, 33]) and numerous *acquisition functions* that balance this trade-off have been proposed [59, 22, 33]. In contrast, the observation-intervention trade-off, which is the focus of this paper, is still relatively unexplored. In the following sections, we formulate this trade-off as an optimal stopping problem and present our main solution approach – *Optimal Stopping for Causal Optimisation*.

#### 4 Optimal stopping formulation of the observation-intervention trade-off

We formulate the problem of designing the sequence of estimation procedures  $(e_t)_{t \in \{1, \dots, T\}}$  as a series of *optimal stopping* problems [66, 54, 47, 16]. In this formulation, we assume that an optimisation policy  $\pi_O$  that inspects the available data and selects the intervention  $\text{do}(\mathbf{X}'_t = \mathbf{x}'_t)$  to evaluate at each stage  $t$ , is given. We place no restrictions on how this policy is obtained or implemented. It may, for example, be derived from an acquisition function that balances the exploration-exploitation trade-off, as is done in e.g. CBO [2]. We further assume that the objective function  $\mu$  (3) and the functions  $\mathbf{F}$  of the underlying SCM are estimated by the probabilistic models  $\hat{\mu}_{\mathbf{D}_t}$  and  $\hat{\mathbf{F}}_{\mathbf{D}_t}$ , respectively. Here  $\mathbf{D}_t$  represents the available data at stage  $t$  of the optimisation and as  $|\mathbf{D}_t| \rightarrow \infty$ ,  $\hat{\mu}_{\mathbf{D}_t} \rightarrow \mu$  and  $\hat{\mathbf{F}}_{\mathbf{D}_t} \rightarrow \mathbf{F}$ .

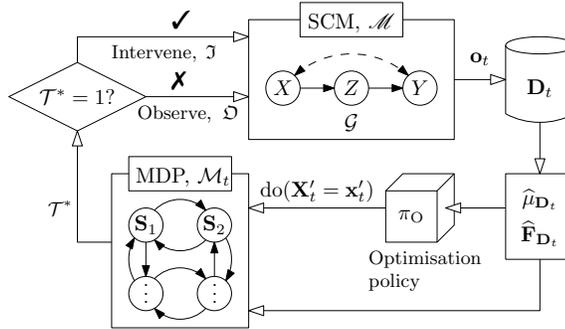


Figure 3: Optimal Stopping for Causal Optimisation (OSCO) to balance the *intervention-observation* trade-off; an optimisation policy  $\pi_O$  decides on a sequence of interventions  $(\text{do}(\mathbf{X}'_t = \mathbf{x}'_t))_{t \in \{1, \dots, T\}}$  to evaluate in an SCM  $\mathcal{M}$  and the procedures to evaluate these interventions are decided by solving optimal stopping problems  $(\mathcal{M}_t)_{t \in \{1, \dots, T\}}$ .

The models  $\hat{\mu}$  and  $\hat{\mathbf{F}}$  allow us to guide the optimisation process and quantify the expected value and uncertainty in different regions of the interventional space (3). Specifically,  $\hat{\mathbf{F}}_{\mathbf{D}_t}$  allows us to estimate causal effects through the do-calculus and  $\hat{\mu}_{\mathbf{D}_t}$  represents the current knowledge of the causal effects, allowing the optimisation policy  $\pi_O$  to make informed decisions about which intervention to evaluate at each stage.

Given the optimisation policy and the probabilistic models defined above, we seek to design the sequence  $(e_t)_{t \in \{1, \dots, T\}}$  to optimally allocate the available evaluation budget between intervening and observing so as to minimise (4a). This task can be formally expressed as a series of Markovian and stationary optimal stopping problems  $\mathcal{M}_1, \dots, \mathcal{M}_T$  (see Fig. 3). To see this, note that, at any stage  $t$  of the optimisation, the models  $\hat{\mu}_{\mathbf{D}_t}$  and  $\hat{\mathbf{F}}_{\mathbf{D}_t}$  allow us to simulate the growth of the dataset  $\mathbf{D}_t$  and plan ahead when deciding between intervening and observing. This look-ahead planning involves two well-known challenges: *i*) the possibly mis-specified models  $\hat{\mu}_{\mathbf{D}_t}$  and  $\hat{\mathbf{F}}_{\mathbf{D}_t}$  may lead to error-propagation when simulating many steps into the future [68]; and *ii*) the number of possible simulation trajectories of  $\mathbf{D}_t$  is infinite, which means that the planning problem corresponds to solving an intractable Markov Decision Process (MDP) [49, 67]. Most existing algorithms deal with these problems by truncating the planning horizon to one step [22, 2, 3, 60]. We propose to instead truncate the planning horizon to the next intervention, which may involve simulating many observation steps. This means that the growth of the dataset  $\mathbf{D}_t$  follows a stationary Markov process governed by the probability law

$$\mathbf{S}_1 \triangleq \mathbf{D}_t, \quad \mathbf{S}_{T+1} \triangleq \perp, \quad \mathbf{S}_{k+1} \triangleq \mathbf{S}_k \cup \{\mathbf{o}_{k+1}, k+1\} \quad (k < T), \quad \mathbf{o}_{k < T} \sim \hat{\mathbf{F}}_{\mathbf{D}_t}(\mathbf{O}_{\mathcal{G}, Y}^{\mathbf{x}'_t}) \quad (5)$$

where  $\mathbf{S}_k \in \mathbf{S}$  denotes the state of the process at time-step  $k$  and  $\perp$  is an absorbing terminal state. At each time-step  $k > 1$  of this process, a new observation  $\mathbf{o}_k$  is sampled from  $\hat{\mathbf{F}}_{\mathbf{D}_t}$  and added to the

dataset  $\mathbf{D}_t \cup \{\mathbf{o}_2, \dots, \mathbf{o}_{k-1}\}$ , which results in a new state  $\mathbf{S}_{k+1}$ . The process is stopped whenever an intervention ( $e_t = \mathfrak{I}$ ) is carried out. Thus the problem of deciding between intervening and observing becomes one of optimal stopping, where the goal is to find an optimal *stopping time*  $\mathcal{T}^*$ :

$$\mathcal{T}^* \in \operatorname{argmax}_{\mathcal{T} \in \{1, \dots, T\}} \left\{ \gamma^{\mathcal{T}-1} r(\mathbf{S}_{\mathcal{T}}) - \sum_{k=1}^{\mathcal{T}-1} \gamma^{k-1} c(\mathbf{X}'_k, \mathfrak{D}) \right\} \quad \text{subject to (4b) - (4c)} \quad (6)$$

where  $\mathcal{T} = \inf\{t : t \geq 1, e_t = \mathfrak{I}\}$  and  $r(\mathbf{S}_{\mathcal{T}})$  denotes the reward of intervening (stopping) at time  $\mathcal{T}$ . Note that if the observation process has not been stopped at time  $k = T - 1$ , the cost constraint in (4b) forces it to stop at time  $T$ , even if no intervention is carried out. We refer the reader to Appendix I for background on optimal stopping theory.

Due to the Markov property, the stopping problem can equivalently be formulated as an MDP and any stopping time that satisfies (6) is also a solution to the following Bellman equation [16, Thm. 3.2]

$$\max_{e_t \in \{\mathfrak{I}, \mathfrak{O}\}} \left\{ r(\mathbf{S}_k), \int \dots \int_{\operatorname{dom}(\mathbf{O}_{\mathcal{G}, Y}^{\mathbf{x}_k})} P_{\widehat{\mathbf{F}}_{\mathbf{D}_t}}(\mathbf{o}_k) V^*(\mathbf{S}_k \cup \{\mathbf{o}_{k+1}\}) d\mathbf{O}_{\mathcal{G}, Y}^{\mathbf{x}_k} - c(\mathbf{X}'_k, \mathfrak{D}) \right\} \quad (7)$$

subject to (4b) - (4c) and (5).

By solving (6), we obtain the optimal stopping time  $\mathcal{T}^*$ , which decides the next evaluation procedure  $e_t$ . In particular, if  $\mathcal{T}^* = 1$ , the causal effect is estimated by intervening ( $e_t = \mathfrak{I}$ ) and otherwise the causal effect is estimated by observing ( $e_t = \mathfrak{O}$ ). In either case, the resulting samples are used to update the probabilistic models  $\widehat{\mu}_{\mathbf{D}_t}$  and  $\widehat{\mathbf{F}}_{\mathbf{D}_t}$  and proceed to the next stage of the optimisation, wherein the next stopping problem  $\mathcal{M}_{t+1}$  is defined. Note that a solution to (6) always exists since  $\mathcal{T}$  is restricted to the finite set  $\{1, \dots, T\}$ , where  $T < \infty$  [16, Thm. 3.2].

**The stopping reward.** A key issue in the design of the above stopping problem is the stopping reward  $r(\mathbf{S}_{\mathcal{T}})$ , which models how beneficial it is to intervene given the state  $\mathbf{S}_{\mathcal{T}}$ . An intervention can be beneficial to the optimisation in two ways. First, it can improve the current estimate of the optimum. Second, it can reduce the uncertainty in the objective function  $\mu$ . We model these two benefits with  $\widehat{\mu}_{\mathbf{S}_k}$  and the *information gain* measure  $I$  [18], respectively:

$$r(\mathbf{S}_{\mathcal{T}}) \triangleq \eta I(\mathbf{S}_k; \mu) \text{ and } r(\mathbf{S}_{k < T}) \triangleq \eta I(\mathbf{S}_k; \mu) - \kappa \widehat{\mu}_{\mathbf{S}_k}(\mathbf{X}'_k, \mathbf{x}'_k) - \tau \frac{\operatorname{Vol}(\mathbf{V})}{\operatorname{Vol}(\mathbf{S}_k)} - c(\mathbf{X}'_k, \mathfrak{I}) \quad (8)$$

Here  $r(\perp) \triangleq 0$  and  $\eta, \tau$  and  $\kappa$  are scalar constants. The information gain  $I(\mathbf{S}_k; \mu) = H(\mathbf{S}_k) - H(\mathbf{S}_k | \mu)$  quantifies the reduction in uncertainty about  $\mu$  from revealing the dataset  $\mathbf{S}_k$ , where  $H$  is the differential entropy function [18, 59]. The terms  $\widehat{\mu}_{\mathbf{S}_k}(\mathbf{X}'_k, \mathbf{x}'_k)$  and  $c(\mathbf{X}'_k, \mathfrak{I})$  quantify the expected value and the cost of the intervention, respectively. Finally,  $\frac{\operatorname{Vol}(\mathbf{V})}{\operatorname{Vol}(\mathbf{S}_k)}$  denotes the convex hull of the interventional domain of  $\mathbf{V}$  divided by the convex hull of the observations in  $\mathbf{S}_k$ . The purpose of this term is to incentivise collection of observations in the beginning of the optimisation when  $|\mathbf{D}_t|$  is small and it is not possible to plan ahead using the models  $\widehat{\mu}$  and  $\widehat{\mathbf{F}}$  (a similar term is used in [2]).

#### 4.1 Efficient computation of the optimal stopping time

Equation (7) implies that it is optimal to intervene (stop) whenever  $r(\mathbf{S}_k) \geq \alpha_{\mathbf{S}_k}$ , where  $\alpha_{\mathbf{S}_k}$  denotes the second expression inside the maximisation in (7). This means that we can divide the state space into two subsets defined by

$$\mathcal{S}_{T-k} \triangleq \{\mathbf{S}_k \mid \mathbf{S}_k \in \mathbf{S}, r(\mathbf{S}_k) \geq \alpha_{\mathbf{S}_k}\} \quad \text{and} \quad \mathcal{C}_{T-k} \triangleq \{\mathbf{S}_k \mid \mathbf{S}_k \in \mathbf{S}, r(\mathbf{S}_k) < \alpha_{\mathbf{S}_k}\} \quad (9)$$

where  $\mathcal{S}_l$  and  $\mathcal{C}_l$  are the stopping and continuation sets with  $l$  time-steps remaining, respectively. These sets cannot overlap and their union  $\mathcal{S}_l \cup \mathcal{C}_l$  covers the state space  $\mathbf{S}$ . Since the set of admissible stopping times in (6) decreases as  $l \rightarrow 1$ , the stopping sets form an increasing sequence  $\mathcal{S}_l \subseteq \mathcal{S}_{l-1} \subseteq \dots \subseteq \mathcal{S}_1$  and similarly the continuation sets form a decreasing sequence  $\mathcal{C}_l \supseteq \mathcal{C}_{l-1} \supseteq \dots \supseteq \mathcal{C}_1$ . Using these sets, the optimal stopping time can be expressed as

$$\mathcal{T}^* = \min \{k \mid k \in \mathbb{N}, \mathbf{S}_{T-k} \in \mathcal{S}_k\} \quad (10)$$

Based on (9)-(10) we state the following structural result regarding the optimal stopping times for the stopping problem defined in (6).

**Theorem 1.** Given the stopping problem in (6), if a) the optimisation policy  $\pi_{\mathcal{O}}$  is such that  $\widehat{\mu}_{\mathcal{S}}(\pi_{\mathcal{O}}(\mathbf{S}))$  is supermodular and  $c(\pi_{\mathcal{O}}(\mathbf{S}), \mathcal{J})$  is non-increasing in  $|\mathcal{S}|$ ; and b)  $I(\mathbf{S}_k; \mu)$  is submodular, then  $\mathcal{S}_1$  is closed. That is,  $P(\mathbf{S}_{k+1} = \mathbf{s}_{k+1} \mid \mathbf{S}_k = \mathbf{s}_k) = 0$  if  $\mathbf{s}_k \in \mathcal{S}_1$  and  $\mathbf{s}_{k+1} \notin \mathcal{S}_1$ .

*Proof.* See Appendix D. □

Informally, Theorem 1 states that if a state  $\mathbf{s}_k$  is encountered for which it is better to intervene than to collect one more observation and then intervene, then no matter the next observation, the next state will always satisfy the same property. This result hinges on two assumptions. Assumption a) states, informally, that as the uncertainty about  $\mu$  is reduced, the optimisation policy  $\pi_{\mathcal{O}}$  explores less and instead prefers exploiting regions of the interventional space that are deemed promising based on  $\widehat{\mu}_{\mathcal{S}}$ . This assumption is for example satisfied by an  $\epsilon$ -greedy optimisation policy with decaying  $\epsilon$ . Similarly, the informal interpretation of assumption b) is that the gain of collecting observations reduces with the number of observations. The conditions for b) to hold are given in [28, Prop. 2] and are true in general. They hold for example if  $\widehat{\mu}_{\mathcal{S}}$  is a Gaussian process (GP) [59].

A direct consequence of Theorem 1 is that the optimal stopping time can be obtained from a simple rule that is efficient to implement in practice, as stated in the following corollary.

**Corollary 1.** If assumptions a) and b) in Theorem 1 hold, then the optimal stopping time is given by

$$\mathcal{T}^* = \min \{k \mid k \in \mathbb{N}, r(\mathbf{S}_k) \geq \mathbb{E}_{\mathbf{o}_{k+1}} [r(\mathbf{S}_k \cup \{\mathbf{o}_{k+1}\})] - c(\mathbf{X}'_t, \mathcal{D})\} \quad (11)$$

and the stopping sets are all equal, i.e.  $\mathcal{S}_1 = \mathcal{S}_2 = \dots = \mathcal{S}_{\mathcal{T}-1}$ .

*Proof.* See Appendix E. □

Corollary 1 states that the stopping problem in (6), which characterises the observation-intervention trade-off for the optimisation problem in (4), permits an optimal solution that is efficient to implement in practical algorithms. In the following sections, we compare this solution to existing approaches and explain how it can be integrated with existing algorithms for optimisation problems with causal structure (e.g. CBO and causal MAB algorithms). The pseudo-code for integrating the optimal stopping problem with the existing algorithms is listed in Algorithm 1 in Appendix H.

## 5 Related work

Problems of optimising decision variables arise in many settings, ranging from the control of physical and computer systems to managing entire economies [49, 48]. Depending on the characteristics of the optimisation problem, different solution methods are appropriate (e.g. convex optimisation [14], dynamic programming [13] and black-box optimisation [33, 22]). We limit the following discussion to related work that studies grey-box optimisation problems with known causal structure. This line of research can be divided into two main approaches: causal BO and causal MABs.

**Causal Bayesian optimisation.** The literature on BO [30, 41] is extensive (see textbook [22] and survey [53]). Most of the prior work on BO is focused on the black-box setting and ignores prior knowledge about the objective function (see the recent tutorial paper by Astudillo & Frazier [5] for examples of prior knowledge). BO problems with known causal structure are usually studied under the aegis of the SCM framework, as is the case in this paper and in [2, 3, 60, 15, 4]. Astudillo & Frazier [5] departs from this idea by instead leveraging function networks in place of SCMs. Another design choice which differ among existing works is the intervention model. This paper studies the hard intervention model, which is consistent with [2, 3, 15], but differ from [5, 60], which study the soft intervention model. Further, all of the existing works (including this paper) except [15, 4] have in common that they assume the causal structure to be known. Branchini et al. [15] and Alabed & Yoneki [4] do not make this assumption and instead explore techniques that combine causal discovery with causal BO.

This work differs from the previous research on causal BO in two main ways. First, we propose a solution to balance the observation-intervention trade-off that emerges in grey-box optimisation problems with causal structure. Existing works either ignore this trade-off or rely on heuristics to balance it. Second, we quantify the costs associated with collecting observations and estimating causal

effects via the do-calculus, which previous works do not (they generally assume that observations can be collected without cost).

**Causal multi-armed bandits.** Non-trivial dependencies amongst bandit arms are typically listed under *structured* bandits. When that structure is explicitly causal the namesake follows [34, 42, 38]. The literature on causal bandits is richer than that of causal BO. Bareinboim et al. [8] were the first to explore the connection between causal reasoning and MAB algorithms. Lattimore et al. [32] and Sen et al. [52] introduced methods for best-arm identification and non-trivial challenges that arise when unobserved confounders (UCs) are present in the SCM, which is explored in [34, 36] where the authors introduce the notion of POMISS for graphs with and without non-manipulative variables respectively. More recently in [64] the authors prove regret bounds for causal MABs with linear SCMs, binary intervention domains and soft interventions. In the listed works thus far, the graph is assumed known. This assumption is relaxed in [39]. Another direction is *budgeted* MABs [40] where pulling an arm comes as a fixed cost and the agent has a finite budget which she has to spend judiciously to find the best arm subject to that limitation.

Similar to the existing work in causal BO, the main differences between this paper and the previous work on causal MAB are a) that we propose a solution to the observation-intervention trade-off; and b) we quantify the costs associated with collecting observations. Further, to our knowledge, ours is the first study that combines the structured and the budgeted MAB approaches.

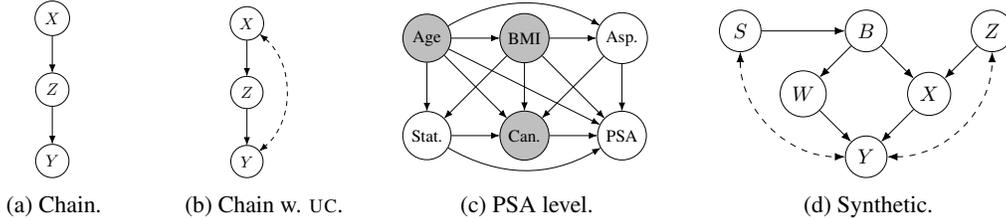


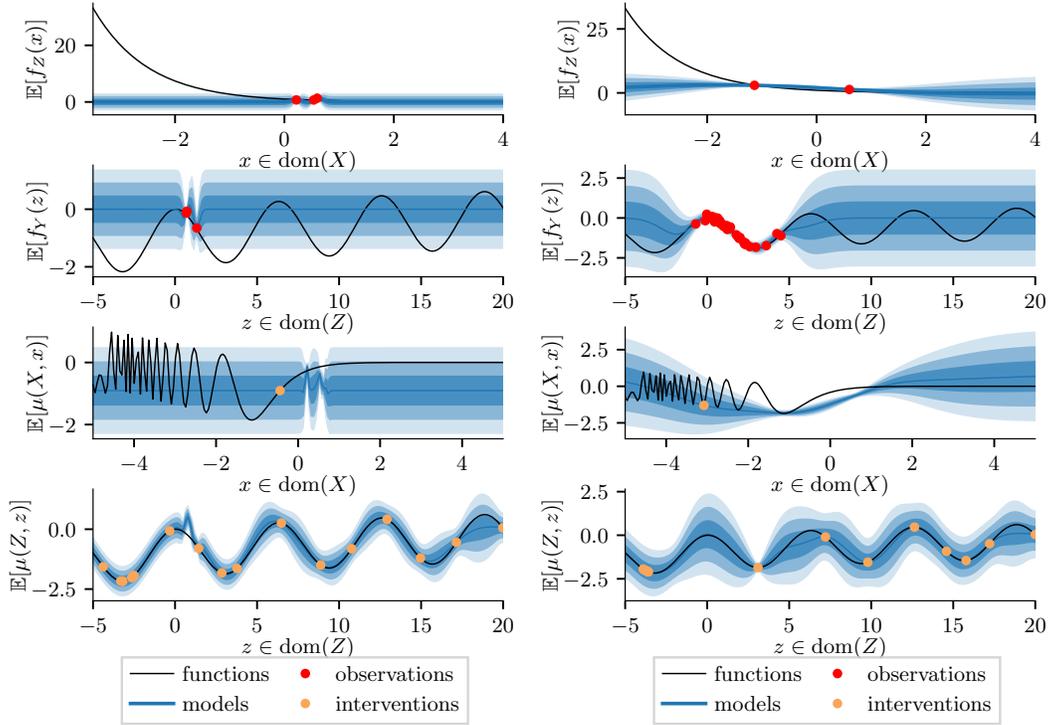
Figure 4: Causal diagrams for the SCMs in the experimental evaluation; non-manipulative variables  $\mathbf{N} \setminus \{Y\}$  are shaded and the outcome variable in each diagram is  $Y \in \mathbf{N}$  apart from Fig. 4c where the outcome variable is the PSA node.

## 6 Experimental evaluation

We integrate OSCO with state-of-the-art algorithms for optimisation problems with causal structure and evaluate these on a variety of synthetic and real-world SCMs with DAGs given in Fig. 4.

**Baselines.** Several algorithms for solving optimisation problems of the type defined in (3) (i.e. optimisation problems with causal structure) have emerged in recent years. These algorithms include CBO [2, Alg. 1], MCBO [60, Alg. 2], DCBO [3, Alg. 1], CEO [15, Alg. 1], the parallel bandit algorithm [31, Alg. 1], causal Thompson sampling [9, 29, Alg. 1], C-UCB [37, Alg. 1] and KL-UCB [35, Alg. 3]. Among these algorithms, we choose to integrate our solution (OSCO) with CBO [2, Alg. 1], MCBO [60, Alg. 2] and C-UCB [37, Alg. 1] as those algorithms are most consistent with our problem setting and assumptions. We leave the integration of OSCO with other algorithms to future work. We also compare OSCO against three heuristic baselines: a) INTERVENE, b) OBSERVE and c) RANDOM, which correspond to policies that a) always intervene, b) always observe and c) selects between intervening and observing randomly. These latter results can be found in the appendices.

**Experiment setup.** We run all experiments with three different random seeds and show the convergence curves of the simple regret metric  $\arg \min_{k \in \{1, \dots, t\}} \mu(\mathbf{X}_k, \mathbf{x}_k) - \mu(\mathbf{X}^*, \mathbf{x}_k^*)$  (3) for  $t = 1, \dots, T$  [22] (this is consistent with the metric reported in [2] but differs from [60, 37] which reports the cumulative regret metric [33]). Hyperparameters are listed in Appendix G and were chosen based on cross-validation. Throughout, we assume that the dataset at the start of the optimisation is empty ( $\mathbf{D}_1 = \emptyset$ ). This contrasts with [2] and [60], which assume  $|\mathbf{D}_1| > 0$  in all experiments. When we compare against CBO we utilise MOS (Def. 4) to reduce the observation costs. We do not utilise MOS when we compare against MCBO as MCBO relies on complete observations. Further, we only evaluate MCBO on the SCMs available in the official implementation [60], namely the chain SCM and



(a) CBO with  $\epsilon$ -greedy (as used in [2]).

(b) CBO with OSCO.

Figure 5: Collected data and estimated models from running CBO with and without OSCO to solve (3) for the chain SCM [2, Fig. 3] (see Fig. 4a); the blue curves and the shaded blue areas show the mean and standard deviation of the estimated models  $\hat{\mathbf{F}}$  and  $\hat{\mu}$ ; the red and orange dots show observations and interventions respectively; the black lines show the SCM functions  $\mathbf{F}$  and the causal effects  $\mu$ .

the PSA SCM. In all implementations of OSCO, we implement the stopping rule implied in Corollary 1 (even in cases when the assumptions of the corollary do not hold, in which case it provides an approximation of the optimal stopping time). Complete experimental details can be found in the appendix.

**Results discussion.** Figure 5 shows the estimated probabilistic models  $\hat{\mu}$  and  $\hat{\mathbf{F}}$  when running CBO with two different policies for balancing the intervention-observation trade-off: *i*) the  $\epsilon$ -greedy policy used in [2]; and *ii*) the OSCO approach described in §4. We note in the lowest plots that the optimal intervention is  $\text{do}(Z = -3.20)$  (with target value  $Y = -2.17$ ) and that this intervention is found in both cases. We further note that CBO with OSCO is able to accurately estimate the interventional distributions through the do-calculus. The main differences between CBO with  $\epsilon$ -greedy and CBO with OSCO are a) CBO with  $\epsilon$ -greedy collects only 3 observations, spending most of the evaluation budget on interventions, whereas CBO with OSCO uses most of the evaluation budget to collect observations; and b) that CBO with  $\epsilon$ -greedy observes all endogenous variables whereas CBO with OSCO only observes the MOS  $\mathbf{O}_{G,Y}^Z = \{Z, Y\}$ . That CBO uses most of the evaluation budget on intervening whereas CBO with OSCO uses most of the budget on observations can be explained by two main reasons. First, the definition of  $\epsilon$  in [2, Eq. 6] implies that the probability of observing in CBO with  $\epsilon$ -greedy is close to 0 when the number of previously collected observations is low. Second, the optimal stopping formulation in (11) implies that CBO with OSCO will observe rather than intervene when it is more cost-effective.

Figure 6 compares OSCO with baselines. The first row in Fig. 6 shows convergence curves of CBO and MCBO with and without OSCO for the chain SCM (Fig. 4a and Fig. 4b – with and without an UC respectively), the synthetic SCM (Fig. 4d) and the PSA SCM (Fig. 4c). An ablation study for different observation costs is shown in the two left-most plots of the second row of Fig. 6. The right-most

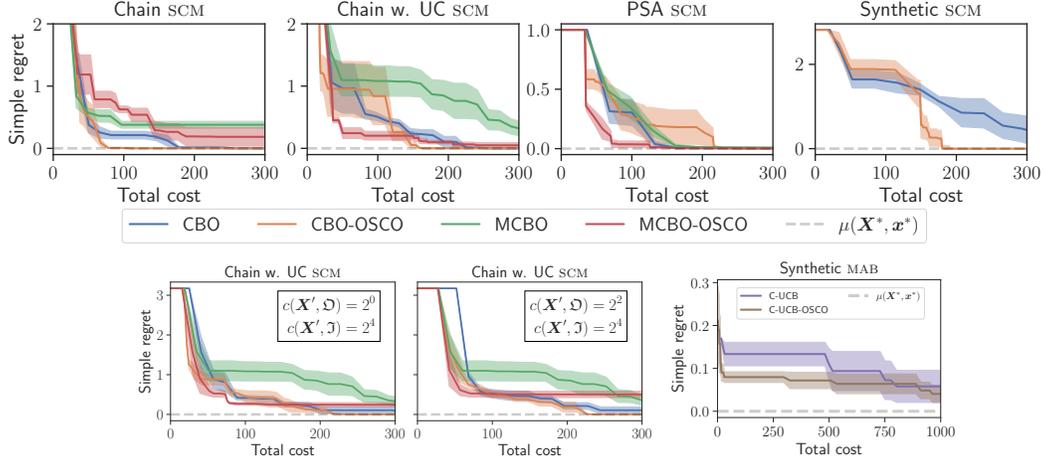


Figure 6: Convergence curves and computational overhead for CBO, MCBO and C-UCB with and without OSCO for different SCMs and causal MABs; the curves indicate the mean and standard deviation ( $\pm \frac{\sigma}{\sqrt{3}}$ ) over three evaluations with different random seeds; the columns from left to right on the **first row** relate to the SCMs in Fig. 4a, Fig. 4b, Fig. 4c and Fig. 4d respectively; the first two columns on the **second row** show convergence curves for different observation costs (all other curves are based on the observation cost  $c(\mathbf{X}', \mathcal{D}) = 2^{-2}$ ) and the right-most column concerns the bandit version of the synthetic SCM in Fig. 4d.

plots in the second row of Fig. 6 show a) converge curves of C-UCB with and without OSCO for the bandit version of the synthetic SCM (Fig. 4d); and b) the computational overhead of OSCO. We note that CBO with OSCO outperforms CBO and finds the optimal intervention for all SCMs within the prescribed evaluation budget. Similarly, we observe that C-UCB with OSCO is more cost-efficient than C-UCB without OSCO for the synthetic SCM. We explain the efficient convergence of OSCO by its design, which a) uses look-ahead-planning to decide between observing and intervening based on what is most cost effective; and b) utilises MOS (Def. 4) to limit the variables that need to be observed. We further note that MCBO with OSCO outperforms MCBO on the chain and PSA SCMs. Moreover, we observe that the performance of CBO is better than that of MCBO on average, which is consistent with the results reported in [60]. This result can be explained by the design of MCBO, which is optimised for the cumulative regret metric rather than the simple regret. Finally, we observe that the computational overhead of OSCO per iteration is less than a factor of 2. Extended evaluation results can be found in Appendix F.

## 7 Conclusion

We have formally defined the observation-intervention trade-off that emerges in optimisation problems with causal structure and have shown that this trade-off can be formulated as a non-myopic optimal stopping problem whose solution determines when a causal effect should be estimated by intervening and when it is more cost-effective to collect observational data. We have also characterised the minimal set of variables that need to be observed to estimate the causal effect – the minimal observation set (MOS). Extensive evaluation results on real and synthetic SCMs show that the optimal stopping formulation can enhance existing algorithms and that the computational overhead is manageable. This paper opens up several directions for future research. One direction is to extend our model to include soft interventions and longer planning horizons. Another direction is to evaluate different reward functions in the optimal stopping problem.

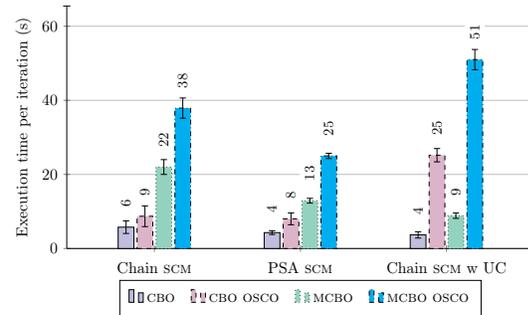


Figure 7: Execution times per iteration with and without OSCO for some of the example SCMs. The height of each bar indicates the mean execution time from 100 measurements and the error bars indicate the standard deviations.

## References

- [1] ABIM Foundation. PSA Blood Test for Prostate Cancer. <https://www.choosingwisely.org/patient-resources/psa-test-for-prostate-cancer/>, 2014. Accessed: 2023-03-23.
- [2] Aglietti, V., Lu, X., Paleyes, A., and González, J. Causal Bayesian Optimization. In *Proceedings of the Twenty Third International Conference on Artificial Intelligence and Statistics*, volume 108 of *Proceedings of Machine Learning Research*, pp. 3155–3164. PMLR, 26–28 Aug 2020.
- [3] Aglietti, V., Dhir, N., González, J., and Damoulas, T. Dynamic Causal Bayesian Optimization. In *Advances in Neural Information Processing Systems*, volume 35, 2021.
- [4] Alabed, S. and Yoneki, E. Bograph: Structured bayesian optimization from logs for expensive systems with many parameters. In *Proceedings of the 2nd European Workshop on Machine Learning and Systems, EuroMLSys '22*, pp. 45–53, New York, NY, USA, 2022. Association for Computing Machinery. ISBN 9781450392549. doi: 10.1145/3517207.3526977.
- [5] Astudillo, R. and Frazier, P. I. Thinking inside the box: A tutorial on grey-box bayesian optimization. In *2021 Winter Simulation Conference (WSC)*, pp. 1–15. IEEE, 2021.
- [6] Bareinboim, E. and Pearl, J. Causal inference by surrogate experiments: z-identifiability. *arXiv preprint arXiv:1210.4842*, 2012.
- [7] Bareinboim, E. and Pearl, J. Causal inference and the data-fusion problem. *Proceedings of the National Academy of Sciences*, 113(27):7345–7352, 2016.
- [8] Bareinboim, E., Forney, A., and Pearl, J. Bandits with unobserved confounders: A causal approach. *Advances in Neural Information Processing Systems*, 28:1342–1350, 2015.
- [9] Bareinboim, E., Forney, A., and Pearl, J. Bandits with unobserved confounders: A causal approach. In Cortes, C., Lawrence, N., Lee, D., Sugiyama, M., and Garnett, R. (eds.), *Advances in Neural Information Processing Systems*, volume 28. Curran Associates, Inc., 2015.
- [10] Bather, J. *Decision Theory: An Introduction to Dynamic Programming and Sequential Decisions*. John Wiley and Sons, Inc., USA, 2000. ISBN 0471976490.
- [11] Bellman, R. A markovian decision process. *Journal of Mathematics and Mechanics*, 6(5): 679–684, 1957.
- [12] Bellman, R. *Dynamic Programming*. Dover Publications, 1957. ISBN 9780486428093.
- [13] Bertsekas, D. P. *Dynamic Programming and Optimal Control*, volume I. Athena Scientific, Belmont, MA, USA, 3rd edition, 2005.
- [14] Boyd, S. and Vandenberghe, L. *Convex Optimization*. Cambridge University Press, March 2004. ISBN 0521833787.
- [15] Branchini, N., Aglietti, V., Dhir, N., and Damoulas, T. Causal entropy optimization. In *Proceedings of The 26th International Conference on Artificial Intelligence and Statistics*, volume 206 of *Proceedings of Machine Learning Research*, pp. 8586–8605. PMLR, 25–27 Apr 2023.
- [16] Chow, Y., Robbins, H., and Siegmund, D. Great expectations: The theory of optimal stopping. In *Journal of the Royal Statistical Society*, 1971.
- [17] Correa, J. and Bareinboim, E. A calculus for stochastic interventions: Causal effect identification and surrogate experiments. In *Proceedings of the AAAI conference on artificial intelligence*, volume 34, pp. 10093–10100, 2020.
- [18] Cover, T. M. and Thomas, J. A. *Elements of Information Theory 2nd Edition (Wiley Series in Telecommunications and Signal Processing)*. Wiley-Interscience, July 2006. ISBN 0471241954.
- [19] Evans, M., Swartz, T., and Swartz, A. *Approximating Integrals Via Monte Carlo and Deterministic Methods*. Oxford statistical science series. Oxford University Press, 2000. ISBN 9780198502784.

- [20] Ferro, A., Pina, F., Severo, M., Dias, P., Botelho, F., and Lunet, N. Use of statins and serum levels of prostate specific antigen. *Acta Urológica Portuguesa*, 32(2):71–77, 2015.
- [21] Frank DiVincenzo, k-health. How much does blood work cost in 2022? <https://khealth.com/learn/healthcare/how-much-does-bloodwork-cost/>, 2022. Accessed: 2023-04-17.
- [22] Garnett, R. *Bayesian Optimization*. Cambridge University Press, 2023. to appear.
- [23] GPyOpt. Gpyopt: A bayesian optimization framework in python. <http://github.com/SheffieldML/GPyOpt>, 2016.
- [24] Hammar, K. and Stadler, R. Intrusion prevention through optimal stopping. *IEEE Transactions on Network and Service Management*, 19(3):2333–2348, 2022. doi: 10.1109/TNSM.2022.3176781.
- [25] Huang, Y. and Valtorta, M. Identifiability in causal bayesian networks: A sound and complete algorithm. In *AAAI*, pp. 1149–1154, 2006.
- [26] Imber, B. S., Varghese, M., Ehdaie, B., and Gorovets, D. Financial toxicity associated with treatment of localized prostate cancer. *Nature Reviews Urology*, 17(1):28–40, 2020.
- [27] Jacqueline Slobin, TalktoMira. What’s the Least Expensive Cholesterol Medication in 2021? <https://www.talktomira.com/post/how-much-do-statins-cost-without-insurance>, 2022-08-22. Accessed: 2023-04-17.
- [28] Krause, A. and Guestrin, C. Near-optimal nonmyopic value of information in graphical models. In *UAI*, pp. 324–331. AUAI Press, 2005. ISBN 0-9749039-1-4.
- [29] Kroon, A. D., Mooij, J., and Belgrave, D. Causal bandits without prior knowledge using separating sets. In Schölkopf, B., Uhler, C., and Zhang, K. (eds.), *Proceedings of the First Conference on Causal Learning and Reasoning*, volume 177 of *Proceedings of Machine Learning Research*, pp. 407–427. PMLR, 11–13 Apr 2022.
- [30] Kushner, H. J. A versatile stochastic model of a function of unknown and time varying form. *Journal of Mathematical Analysis and Applications*, 5(1):150–167, 1962. ISSN 0022-247X. doi: [https://doi.org/10.1016/0022-247X\(62\)90011-2](https://doi.org/10.1016/0022-247X(62)90011-2).
- [31] Lattimore, F., Lattimore, T., and Reid, M. D. Causal bandits: Learning good interventions via causal inference. In *Proceedings of the 30th International Conference on Neural Information Processing Systems, NIPS’16*, pp. 1189–1197, Red Hook, NY, USA, 2016. Curran Associates Inc. ISBN 9781510838819.
- [32] Lattimore, F., Lattimore, T., and Reid, M. D. Causal bandits: Learning good interventions via causal inference. In *Advances in Neural Information Processing Systems*, pp. 1181–1189, 2016.
- [33] Lattimore, T. and Szepesvári, C. *Bandit algorithms*. Cambridge University Press, 2020.
- [34] Lee, S. and Bareinboim, E. Structural causal bandits: where to intervene? *Advances in Neural Information Processing Systems*, 31, 2018.
- [35] Lee, S. and Bareinboim, E. Structural causal bandits with non-manipulable variables. *Proceedings of the AAAI Conference on Artificial Intelligence*, 33(01):4164–4172, Jul. 2019. doi: 10.1609/aaai.v33i01.33014164.
- [36] Lee, S. and Bareinboim, E. Characterizing optimal mixed policies: Where to intervene and what to observe. *Advances in neural information processing systems*, 33, 2020.
- [37] Lu, Y., Meisami, A., Tewari, A., and Yan, W. Regret analysis of bandit problems with causal background knowledge. In Peters, J. and Sontag, D. (eds.), *Proceedings of the 36th Conference on Uncertainty in Artificial Intelligence (UAI)*, volume 124 of *Proceedings of Machine Learning Research*, pp. 141–150. PMLR, 03–06 Aug 2020.

- [38] Lu, Y., Meisami, A., Tewari, A., and Yan, W. Regret analysis of bandit problems with causal background knowledge. In *Conference on Uncertainty in Artificial Intelligence*, pp. 141–150. PMLR, 2020.
- [39] Lu, Y., Meisami, A., and Tewari, A. Causal bandits with unknown graph structure. *Advances in Neural Information Processing Systems*, 34:24817–24828, 2021.
- [40] Madani, O., Lizotte, D. J., and Greiner, R. The budgeted multi-armed bandit problem. In *International Conference on Computational Learning Theory*, pp. 643–645. Springer, 2004.
- [41] Močkus, J. On bayesian methods for seeking the extremum. In Marchuk, G. I. (ed.), *Optimization Techniques IFIP Technical Conference Novosibirsk, July 1–7, 1974*, pp. 400–404, Berlin, Heidelberg, 1975. Springer Berlin Heidelberg. ISBN 978-3-540-37497-8.
- [42] Nair, V., Patil, V., and Sinha, G. Budgeted and non-budgeted causal bandits. In *International Conference on Artificial Intelligence and Statistics*, pp. 2017–2025. PMLR, 2021.
- [43] Pate, S. C., Uhlman, M. A., Rosenthal, J. A., Cram, P., and Erickson, B. A. Variations in the open market costs for prostate cancer surgery: a survey of US hospitals. *Urology*, 83(3): 626–631, 2014.
- [44] Pearl, J. *Causality: Models, Reasoning and Inference*. Cambridge University Press, USA, 2nd edition, 2009.
- [45] Pearl, J. *Causality: models, reasoning and inference*. Cambridge university press, 2009.
- [46] Pearl, J. and Robins, J. M. Probabilistic evaluation of sequential plans from causal models with hidden variables. In *UAI*, volume 95, pp. 444–453. Citeseer, 1995.
- [47] Peskir, G. and Shiryaev, A. *Optimal stopping and free-boundary problems*. Lectures in mathematics (ETH Zürich). Springer, 2006.
- [48] Powell, W. B. *Approximate Dynamic Programming: Solving the Curses of Dimensionality*. Wiley Series in Probability and Statistics. Wiley, Hoboken, NJ, USA, 2nd edition, 2011.
- [49] Puterman, M. L. *Markov Decision Processes: Discrete Stochastic Dynamic Programming*. John Wiley and Sons, Inc., USA, 1st edition, 1994. ISBN 0471619779.
- [50] Ross, S. M. *Introduction to Stochastic Dynamic Programming: Probability and Mathematical*. Academic Press, Inc., USA, 1983. ISBN 0125984200.
- [51] Rubinstein, R. Y. and Kroese, D. P. *Simulation and the Monte Carlo Method*. Wiley Publishing, 3rd edition, 2016. ISBN 1118632168.
- [52] Sen, R., Shanmugam, K., Dimakis, A. G., and Shakkottai, S. Identifying best interventions through online importance sampling. In *International Conference on Machine Learning*, pp. 3057–3066. PMLR, 2017.
- [53] Shahriari, B., Swersky, K., Wang, Z., Adams, R. P., and De Freitas, N. Taking the human out of the loop: A review of bayesian optimization. *Proceedings of the IEEE*, 104(1):148–175, 2015.
- [54] Shirayev, A. N. *Optimal Stopping Rules*. Springer-Verlag Berlin, 2007. Reprint of russian edition from 1969.
- [55] Shpitser, I. and Pearl, J. Identification of conditional interventional distributions. In *Proceedings of the Twenty-Second Conference on Uncertainty in Artificial Intelligence*, pp. 437–444, Arlington, Virginia, USA, 2006. AUAI Press.
- [56] Shpitser, I. and Pearl, J. Identification of joint interventional distributions in recursive semi-markovian causal models. In *Proceedings of the 21st National Conference on Artificial Intelligence*, volume 2, pp. 1219–1226. AAAI Press, 2006.
- [57] Shpitser, I. and Pearl, J. Complete identification methods for the causal hierarchy. *Journal of Machine Learning Research*, 9(9), 2008.

- [58] Snell, J. L. Applications of martingale system theorems. *Transactions of the American Mathematical Society*, 73:293–312, 1952.
- [59] Srinivas, N., Krause, A., Kakade, S. M., and Seeger, M. W. Information-theoretic regret bounds for gaussian process optimization in the bandit setting. *IEEE Transactions on Information Theory*, 58(5):3250–3265, 2012.
- [60] Sussex, S., Makarova, A., and Krause, A. Model-based causal bayesian optimization, 2022.
- [61] Tian, J. and Pearl, J. A general identification condition for causal effects. In *Eighteenth National Conference on Artificial Intelligence*, volume 18, pp. 567–573, 2002.
- [62] Tikka, S. and Karvanen, J. Identifying causal effects with the r package causaleffect. *arXiv preprint arXiv:1806.07161*, 2018.
- [63] Tikka, S., Hyttinen, A., and Karvanen, J. Causal effect identification from multiple incomplete data sources: A general search-based approach. *Journal of Statistical Software*, 99(5):1–40, 2021.
- [64] Varici, B., Shanmugam, K., Sattigeri, P., and Tajer, A. Causal bandits for linear structural equation models. *arXiv preprint arXiv:2208.12764*, 2022.
- [65] Vives, X. Nash equilibrium with strategic complementarities. *Journal of Mathematical Economics*, 19(3):305–321, 1990. ISSN 0304-4068. doi: [https://doi.org/10.1016/0304-4068\(90\)90005-T](https://doi.org/10.1016/0304-4068(90)90005-T). URL <https://www.sciencedirect.com/science/article/pii/030440689090005T>.
- [66] Wald, A. *Sequential Analysis*. Wiley and Sons, New York, 1947.
- [67] Wu, J. and Frazier, P. Practical two-step lookahead bayesian optimization. In Wallach, H., Larochelle, H., Beygelzimer, A., d Alché-Buc, F., Fox, E., and Garnett, R. (eds.), *Advances in Neural Information Processing Systems*, volume 32. Curran Associates, Inc., 2019.
- [68] Yue, X. and Kontar, R. A. Why non-myopic bayesian optimization is promising and how far should we look-ahead? a study via rollout. In Chiappa, S. and Calandra, R. (eds.), *Proceedings of the Twenty Third International Conference on Artificial Intelligence and Statistics*, volume 108 of *Proceedings of Machine Learning Research*, pp. 2808–2818. PMLR, 26–28 Aug 2020.

## Contents

<b>1</b>	<b>Introduction</b>	<b>1</b>
<b>2</b>	<b>Theoretical background</b>	<b>2</b>
2.1	Structural causal models . . . . .	2
2.2	Sets of endogenous variables . . . . .	3
<b>3</b>	<b>Problem statement</b>	<b>4</b>
<b>4</b>	<b>Optimal stopping formulation of the observation-intervention trade-off</b>	<b>5</b>
4.1	Efficient computation of the optimal stopping time . . . . .	6
<b>5</b>	<b>Related work</b>	<b>7</b>
<b>6</b>	<b>Experimental evaluation</b>	<b>8</b>
<b>7</b>	<b>Conclusion</b>	<b>10</b>
	<b>Appendices</b>	<b>16</b>
	<b>Appendix A Notation</b>	<b>16</b>
	<b>Appendix B Modelling assumptions</b>	<b>17</b>
	<b>Appendix C Causal-effect derivation</b>	<b>18</b>
	<b>Appendix D Proof of Theorem 1</b>	<b>19</b>
	<b>Appendix E Proof of Corollary 1</b>	<b>19</b>
	<b>Appendix F Additional evaluation results</b>	<b>19</b>
F.1	Chain SCM . . . . .	20
F.2	Chain SCM with an unobserved confounder . . . . .	21
F.3	PSA SCM . . . . .	22
F.4	Synthetic SCM . . . . .	22
	<b>Appendix G Hyperparameters</b>	<b>26</b>
G.1	Hyperparameters for the chain SCM . . . . .	27
G.2	Hyperparameters for the chain SCM with an unobserved confounder . . . . .	27
G.3	Hyperparameters for the synthetic example SCM . . . . .	28
G.4	Hyperparameters for the PSA SCM . . . . .	30
G.5	Synthetic causal MAB . . . . .	31
	<b>Appendix H Pseudocode and implementation of OSCO</b>	<b>31</b>

<b>Appendix I</b>	<b>Background on Markovian optimal stopping problems</b>	<b>32</b>
I.1	Markov decision processes . . . . .	33
I.2	Markovian optimal stopping problems . . . . .	33

# Appendices

## Appendix A Notation

Random variables are denoted by upper-case letters (e.g.  $X$ ) and their values by lower-case letters (e.g.  $x$ ). The probability mass or density of a random variable  $X$  is denoted by  $P(X)$ . We use  $x \sim P(X)$  to denote that  $x$  was sampled from  $P(X)$ . The expectation of a function  $f$  with respect to a random variable  $X$  is denoted by  $\mathbb{E}_X[f]$ . Sets of variables and their values are noted by bold upper-case and lower-case letters respectively (e.g.  $\mathbf{x}$  and  $\mathbf{X}$ ). Operators, function spaces and tuples are represented with upper case calligraphic letters (e.g.  $\mathcal{M}$ ). The power set of a set  $\mathbf{X}$  is denoted with  $\mathcal{P}(\mathbf{X})$ . The set of all probability distributions over a set  $\mathbf{X}$  (i.e. the  $(|\mathbf{X}| - 1)$ -dimensional unit simplex) is denoted with  $\Delta(\mathbf{X})$ . We make extensive use of the do-calculus (for details see [45, §3.4]). The domain of a variable is denoted by  $\text{dom}(\cdot)$  where e.g.  $x \in \text{dom}(X)$  and  $\mathbf{x} \in \text{dom}(\mathbf{X}) \equiv x_1 \times x_2 \times \dots \times x_{|\mathbf{x}|} \in \text{dom}(X_1) \times \text{dom}(X_2) \times \dots \times \text{dom}(X_{|\mathbf{x}|})$ . The set of real numbers and the set of  $n$ -dimensional real vectors are denoted with  $\mathbb{R}$  and  $\mathbb{R}^n$  respectively. We adopt family relationships  $\text{pa}(X)_{\mathcal{G}}$ ,  $\text{ch}(X)_{\mathcal{G}}$ ,  $\text{an}(X)_{\mathcal{G}}$  and  $\text{de}(X)_{\mathcal{G}}$  to denote parents, children, ancestors and descendants of a given variable  $X$  in a graph  $\mathcal{G}$ ; Pa, Ch, An and De extends pa, ch, an and de by including the argument as the result. For example  $\text{Pa}(X)_{\mathcal{G}} = \text{pa}(X)_{\mathcal{G}} \cup \{X\}$ . With a set of variables as argument,  $\text{pa}(\mathbf{X})_{\mathcal{G}} = \bigcup_{X \in \mathbf{X}} \text{pa}(X)_{\mathcal{G}}$  and similarly defined for other relations.

Table 1: Notation used throughout the paper.

Notation(s)	Description
$\mathcal{M}$	quadruple defining an SCM $\mathcal{M} = \langle \mathbf{U}, \mathbf{V}, \mathbf{F}, P(\mathbf{U}) \rangle$
$\mathbf{V}$	set of endogeneous variables in an SCM
$\mathbf{U}$	set of exogeneous variables in an SCM
$\mathbf{Y}$	set of target variables in an SCM
$\mathbf{X}$	set of manipulative variables in an SCM
$\mathbf{N}$	set of non-manipulative variables in an SCM
$\mathbf{F}$	structural equation model of an SCM
$\mathcal{G}$	causal diagram (DAG) of an SCM (with nodes $\mathbf{V}$ )
$\mathbf{E}$	edges of $\mathcal{G}$
$\text{do}(\mathbf{X} = \mathbf{x})$	the do-operator [45]
$\mathcal{G}_{\overline{\mathbf{X}}}$	the mutilated graph obtained by deleting from $\mathcal{G}$ all arcs pointing to nodes in $\mathbf{X}$
$\mathbf{M}_{\mathcal{G}, Y}^{\mathbf{V}}$	set of MISS (Def. 2) for an SCM with endogeneous variables $\mathbf{V}$ and target variable $Y$
$\mathbf{P}_{\mathcal{G}, Y}^{\mathbf{V}}$	set of POMISS (Def. 3) for an SCM with endogeneous variables $\mathbf{V}$ and target variable $Y$
$\mathbf{O}_{\mathcal{G}, Y}^{\mathbf{X}}$	MOS (Def. 4) for an identifiable intervention $P(Y   \text{do}(\mathbf{X} = \mathbf{x}))$
$Q_Y^{\mathbf{X}}$	do-calculus expression to estimate $P(Y   \text{do}(\mathbf{X} = \mathbf{x}))$ from $P(\mathbf{V})$
$\mu(\mathbf{X}', \mathbf{x}')$	shorthand for $\mathbb{E}[Y   \text{do}(\mathbf{X}' = \mathbf{x}')]$
$\mathbf{X}^*, \mathbf{x}^*$	optimal intervention set $\mathbf{X}^*$ and intervention levels $\mathbf{x}^*$
$e$	estimation procedure, $e \in \{\mathcal{I}, \mathcal{O}\}$
$\mathcal{I}$	estimation by intervention
$\mathcal{O}$	estimation by observation
$c(\mathbf{X}', e)$	cost of estimating $\mathbb{E}[Y   \text{do}(\mathbf{X}' = \mathbf{x}')] using procedure e \in \{\mathcal{I}, \mathcal{O}\}$
$T$	time horizon of the optimisation
$K$	maximum evaluation cost
$\mathbf{D}_t$	dataset of measured observations and interventions at stage $t$ of the optimisation
$\widehat{\mu}_{\mathbf{D}_t}$	probabilistic model of $\mu$ based on $\mathbf{D}_t$
$\widehat{\mathbf{F}}_{\mathbf{D}_t}$	probabilistic model of $\mathbf{F}$ based on $\mathbf{D}_t$
$\mathcal{M}_t$	stopping problem at stage $t$ of the optimisation
$\mathbf{S}_k, \mathbf{o}_k$	state and observation at stage $k$ of an optimal stopping problem
$\perp$	terminal state of an optimal stopping problem
$r(\mathbf{S}_k)$	stopping reward at stage $k$ of an optimal stopping problem
$\mathcal{T}$	stopping time
$\gamma$	discount factor for an optimal stopping problem
$\mathcal{S}, \mathcal{C}$	stopping and continuation sets for an optimal stopping problem

## Appendix B Modelling assumptions

This sections contains two tables which detail our modelling assumptions on the causal inference and optimal stopping sides respectively.

Table 2: Causal inference assumptions.

Assumption	Description
$ \mathbf{V}  < \infty$	the set of endogenous variables is finite
univariate target $Y \in \mathbf{V}$	we do not consider multivariate targets $\mathbf{Y} \subset \mathbf{V},  \mathbf{Y}  > 1$
target $Y \in \mathbf{V}$ is bounded	$ y  \leq M < \infty$ for some $M \in \mathbb{R}$ and all $y \in \text{dom}(Y)$
atomic interventions	interventions $\text{do}(\mathbf{X}' = \mathbf{x}')$ in (3) are atomic [17]
stationary DAG topology	the DAG topology is independent of time $t$
stationary $\mathbf{F}$	the functions $f_i \in \mathbf{F}$ are independent of time $t$
$\mathcal{G}$ is a DAG	causal diagrams are free of cycles
identifiability methods	methods based on $P(\mathbf{V})$ only (i.e. non-experimental [63, Table 1])

Table 3: Optimal stopping assumptions.

Assumption	Description
$c(\mathbf{L}, \mathcal{D}) > 0 \forall \mathbf{L} \in \mathcal{P}(\mathbf{V})$	positive observation costs
$c(\mathbf{M}, \mathcal{J}) > 0 \forall \mathbf{M} \in \mathcal{P}(\mathbf{V})$	positive intervention costs
$c(\mathbf{X}', \mathcal{D}) < M < \infty \forall \mathbf{L} \in \mathcal{P}(\mathbf{V})$	bounded observation costs ( $M \in \mathbb{R}$ )
$c(\mathbf{X}', \mathcal{J}) < M < \infty \forall \mathbf{M} \in \mathcal{P}(\mathbf{X})$	bounded intervention costs ( $M \in \mathbb{R}$ )
$T < \infty$	finite time horizon $\implies \mathcal{T}^* < \infty$ (6)

## Appendix C Causal-effect derivation

Derivation [7] for estimating the causal effect of  $X$  on  $Y$  in Fig. 1a. We use the shorthand  $P_X(Y)$  here to denote the interventional distribution  $P(Y \mid \text{do}(X = x))$ . See [45, Thm. 3.4.1] for the three rules of do-calculus.

*Proof.* Summing over  $Z$  gives

$$P_X(Y) = \sum_Z P_X(Y, Z) \quad (12)$$

By C-component factorisation, we have

$$= \sum_Z P_{X,Y}(Z) P_{X,Z}(Y) \quad (13)$$

**Task 1: Compute  $P_{X,Y}(Z)$**

The third rule of do-calculus can be applied using the independence  $(Y \perp Z \mid X)_{\mathcal{G}_{\overline{X,Y}}}$  (see Fig. 1).

$$P_{X,Y}(Z) = P_X(Z) \quad (14)$$

The second rule of do-calculus can be applied using the independence  $(X \perp Z)_{\mathcal{G}_{\overline{X}}}$  (see Fig. 1).

$$= P(Z \mid X) \quad (15)$$

**Task 2: Compute  $P_{X,Z}(Y)$**

The third rule of do-calculus can be applied using the independence  $(X \perp Y \mid Z)_{\mathcal{G}_{\overline{X,Z}}}$  (see Fig. 1).

$$P_{X,Z}(Y) = P_Z(Y) \quad (16)$$

Summing over  $X'$  gives

$$= \sum_{X'} P_Z(X', Y) \quad (17)$$

**Task 2.1: Compute  $P_Z(X', Y)$**

We compute the effect inside the sum. By the chain rule, we have

$$P_Z(X', Y) = P_Z(Y \mid X') P_Z(X') \quad (18)$$

The third rule of do-calculus can be applied using the independence  $(Z \perp X')_{\mathcal{G}_{\overline{Z}}}$  (see Fig. 1).

$$= P_Z(Y \mid X') P(X') \quad (19)$$

The second rule of do-calculus can be applied using the independence  $(Z \perp Y \mid X')_{\mathcal{G}_{\overline{Z}}}$  (refer to Fig. 1).

$$= P(Y \mid X', Z) P(X') \quad (20)$$

Substituting (15) and (20) back into (13), we get

$$P_X(Y) = \sum_Z P(Z \mid X) \sum_{X'} P(Y \mid X', Z) P(X') \quad (21)$$

□

## Appendix D Proof of Theorem 1

*Proof.* For ease of notation, let  $\mu_{\mathbf{S}_k}$ ,  $c_{\mathcal{D}}$ , and  $V_{\mathbf{S}_k}$  be a shorthands for  $\mu_{\mathbf{S}_k}(\mathbf{X}'_k, \mathbf{x}'_k)$ ,  $c(\mathbf{X}'_t, \mathcal{D})$ , and  $\frac{\text{Vol}(\mathbf{V})}{\text{Vol}(\mathbf{S}_k)}$ , respectively.

$$\mathbf{S}_k \in \mathcal{S}_1 \quad (22)$$

$$\implies r(\mathbf{S}_k) \geq \mathbb{E}_{\mathbf{o}_{k+1}} [r(\mathbf{S}_k \cup \{\mathbf{o}_{k+1}\})] - c_{\mathcal{D}} \quad (23)$$

$$\iff \eta I(\mathbf{S}_k; \mu) - \kappa \widehat{\mu}_{\mathbf{S}_k} - \tau V_{\mathbf{S}_k} \geq \mathbb{E}_{\mathbf{o}_{k+1}} [\eta I(\mathbf{S}_{k+1}; \mu) - \kappa \widehat{\mu}_{\mathbf{S}_{k+1}} - \tau V_{\mathbf{S}_{k+1}}] - c_{\mathcal{D}} \quad (24)$$

$$\implies \eta I(\mathbf{S}_k; \mu) - \kappa \widehat{\mu}_{\mathbf{S}_k} \geq \mathbb{E}_{\mathbf{o}_{k+1}} [\eta I(\mathbf{S}_{k+1}; \mu) - \kappa \widehat{\mu}_{\mathbf{S}_{k+1}}] - c_{\mathcal{D}} \quad (25)$$

$$\implies \kappa (\mathbb{E}_{\mathbf{o}_{k+1}} [\widehat{\mu}_{\mathbf{S}_{k+1}}] - \widehat{\mu}_{\mathbf{S}_k}) \geq \eta (\mathbb{E}_{\mathbf{o}_{k+1}} [I(\mathbf{S}_{k+1}; \mu)] - I(\mathbf{S}_k; \mu)) - c_{\mathcal{D}} \quad (26)$$

$$\implies \kappa (\mathbb{E}_{\mathbf{o}_{k+2}} [\widehat{\mu}_{\mathbf{S}_{k+1}}] - \widehat{\mu}_{\mathbf{S}_k}) \geq \eta (\mathbb{E}_{\mathbf{o}_{k+1}} [I(\mathbf{S}_{k+1}; \mu)] - I(\mathbf{S}_k; \mu)) - c_{\mathcal{D}} \quad (27)$$

$$\implies \kappa (\mathbb{E}_{\mathbf{o}_{k+2}} [\widehat{\mu}_{\mathbf{S}_{k+2}}] - \widehat{\mu}_{\mathbf{S}_{k+1}}) \geq \eta (\mathbb{E}_{\mathbf{o}_{k+1}} [I(\mathbf{S}_{k+1}; \mu)] - I(\mathbf{S}_k; \mu)) - c_{\mathcal{D}} \quad (28)$$

$$\implies \kappa (\mathbb{E}_{\mathbf{o}_{k+2}} [\widehat{\mu}_{\mathbf{S}_{k+2}}] - \widehat{\mu}_{\mathbf{S}_{k+1}}) \geq \eta (\mathbb{E}_{\mathbf{o}_{k+2}} [I(\mathbf{S}_{k+1}; \mu)] - I(\mathbf{S}_k; \mu)) - c_{\mathcal{D}} \quad (29)$$

$$\implies \kappa (\mathbb{E}_{\mathbf{o}_{k+2}} [\widehat{\mu}_{\mathbf{S}_{k+2}}] - \widehat{\mu}_{\mathbf{S}_{k+1}}) \geq \eta (\mathbb{E}_{\mathbf{o}_{k+2}} [I(\mathbf{S}_{k+2}; \mu)] - I(\mathbf{S}_{k+1}; \mu)) - c_{\mathcal{D}} \quad (30)$$

$$\implies \mathbf{S}_{k+1} \in \mathcal{S}_1 \quad (31)$$

Equation (23) follows from the Bellman equation (7) and (24) follows because  $c(\pi_{\mathcal{O}}(\mathbf{S}), \mathcal{J})$  is non-increasing in  $|\mathbf{S}|$ , which is implied by assumption a). Equation (25) holds because  $\frac{\text{Vol}(\mathbf{V})}{\text{Vol}(\mathbf{S}_k)} \geq \frac{\text{Vol}(\mathbf{V})}{\text{Vol}(\mathbf{S}_{k+1})}$  by definition. Equation (26) follows from linearity of  $\mathbb{E}$ . Equation (27) follows from stationarity of the observation distribution  $\widehat{P}_{\mathbf{S}_t}$ . Equation (28) follows from supermodularity of  $\widehat{\mu}_{\mathbf{S}}$  (which is preserved by integration [65]), i.e.  $\widehat{\mu}_{\mathbf{S}_k \cup \mathbf{o}_{k+2}} - \widehat{\mu}_{\mathbf{S}_k} \leq \widehat{\mu}_{\mathbf{S}_{k+1} \cup \mathbf{o}_{k+2}} - \widehat{\mu}_{\mathbf{S}_{k+1}}$ , which is implied by assumption a) and  $\mathbf{S}_k \subset \mathbf{S}_{k+1}$ . Similarly, (29) and (30) follows from stationarity of  $\widehat{P}_{\mathbf{S}_t}$  and submodularity of  $I$ , respectively. More specifically, (30) holds because  $\mathbf{S}_k \subset \mathbf{S}_{k+1}$  and  $I(\mathbf{S}_k \cup \{\mathbf{o}_{k+2}\}; \mu) - I(\mathbf{S}_k; \mu) \geq I(\mathbf{S}_{k+1} \cup \{\mathbf{o}_{k+2}\}; \mu) - I(\mathbf{S}_{k+1}; \mu)$ , which is implied by assumption b). Finally, (31) follows from (7).  $\square$

## Appendix E Proof of Corollary 1

*Proof.* The corollary follows from a well-known result in optimal stopping theory (see [13, pp. 147-149] and [10, Prop. 7.3]). The rule in (11) is known as a *one-step lookahead policy*. To prove (11) we note that, by definition of  $\mathcal{S}_1$ , (11) holds if  $k = T - 1$ . Assume by induction that (11) holds for some integer  $n + 1 < T - 1$  and consider a state  $\mathbf{S}_n \in \mathcal{S}_1$ . Then

$$\mathcal{T}^* = n \iff r(\mathbf{S}_n) \geq \mathbb{E}_{\mathbf{o}_{n+1}} [V^*(\mathbf{S}_{n+1})] - c(\mathbf{X}'_t, \mathcal{D}) \quad (32)$$

$$= \mathbb{E}_{\mathbf{o}_{n+1}} [r(\mathbf{S}_{n+1})] - c(\mathbf{X}'_t, \mathcal{D}) \quad (33)$$

$$\leq r(\mathbf{S}_n) \quad (34)$$

$$\implies \mathbf{S}_n \in \mathcal{S}_n \quad (35)$$

where (32) follows from the Bellman equation (7) and (33) follows from Theorem 1 and the fact that  $\mathcal{S}_1$  is closed. We then have, by induction and by (35), that  $\mathbf{S}' \in \mathcal{S}_1 \implies \mathbf{S}' \in \mathcal{S}_l$ , for all  $l \in \{1, \dots, T - 1\}$ . Then, since  $\mathcal{S}_l \subseteq \mathcal{S}_{l-1} \subseteq \dots \subseteq \mathcal{S}_1$  by definition, we have that  $\mathcal{S}_1 = \mathcal{S}_2 = \dots = \mathcal{S}_{T-1}$ , which directly implies (11).  $\square$

## Appendix F Additional evaluation results

This appendix contains additional evaluation results, complementing those in the main body of the paper. Appendix F.1 contains results for the chain SCM (see Fig. 4a); Appendix F.2 contains results for the chain SCM with an unobserved confounder (see Fig. 4b); Appendix F.3 contains results for the PSA SCM (see Fig. 4c); and Appendix F.4 contains results for the synthetic SCM with causal graph in Fig. 2.

To re-emphasise, in all experiments, we only explore the POMISS for each SCM – for a complete pseudo-algorithm see Algorithm 1.

## E.1 Chain SCM

The chain SCM (see Fig. 4a) is a synthetic SCM that is benchmarked in both [2] and [60]. Figure 5 and Fig. 8 show the estimated probabilistic models  $\hat{\mu}$  and  $\hat{\mathbf{F}}$  when running CBO with four different policies for balancing the intervention-observation trade-off: *i*) the  $\epsilon$ -greedy policy used in [2]; *ii*) the OSCO approach described in §4; *iii*) the OBSERVE baseline (which always observes); and *iv*) the RANDOM baseline, which selects between intervening and observing uniformly at random.

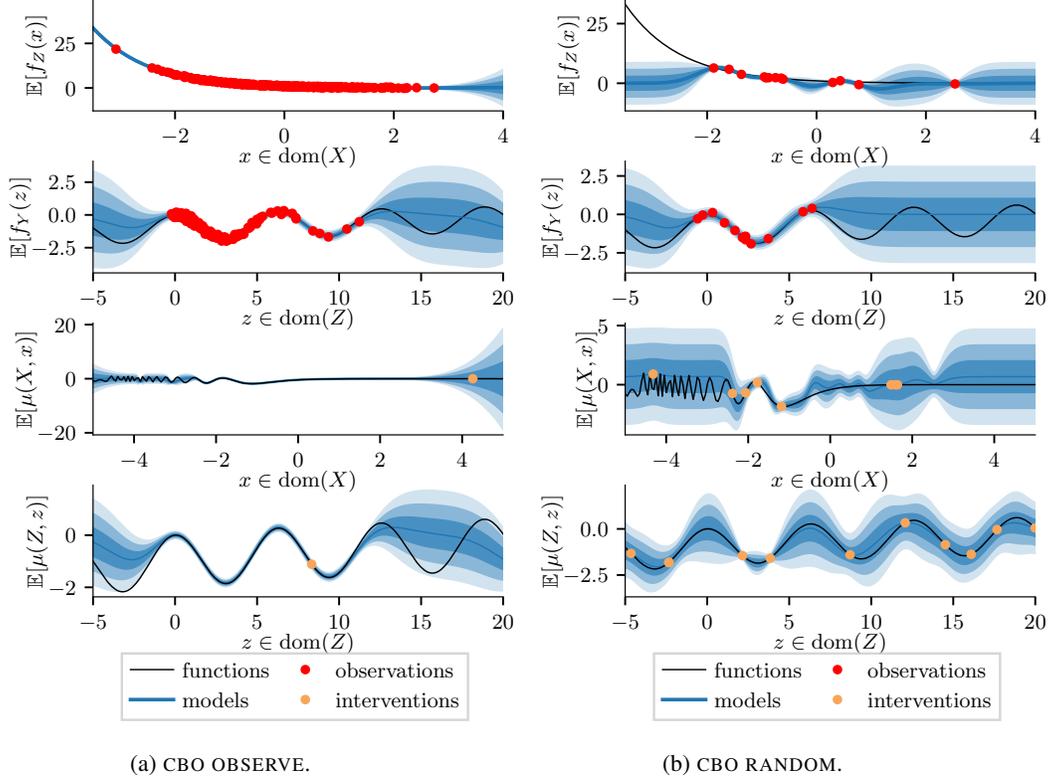


Figure 8: Collected data and estimated models from running CBO to solve (3) for the chain SCM [2, Fig. 3] (see Fig. 4a); the left plot (Fig. 8a) shows results when using a policy that always observes and the right plot (Fig. 8b) shows results when using a policy that selects randomly between observing and intervening; the blue curves and the shaded blue areas show the mean and standard deviation of the estimated models  $\hat{\mathbf{F}}$  and  $\hat{\mu}$ ; the red and orange dots show observations and interventions; the black lines show the SCM functions  $\mathbf{F}$  and the causal effects  $\mu$ .

We note in the lowest plots that the optimal intervention is  $\text{do}(Z = -3.20)$  (with target value  $Y = -2.17$ ) and that this intervention is found in all cases except for the OBSERVE baseline (Fig. 8a). That the OBSERVE baseline does not find the optimal intervention is expected as the probability of observing the optimal configuration without intervening is low. We further note that all policies that collect observations are able to accurately estimate the interventional distributions through the do-calculus (see e.g. Fig. 8a and Fig. 5b). The main differences between CBO with  $\epsilon$ -greedy and CBO with OSCO (see Fig. 5) are a) CBO with  $\epsilon$ -greedy collects only 3 observations, spending most of the evaluation budget on interventions, whereas CBO with OSCO uses most of the evaluation budget to collect observations; and b) that CBO with  $\epsilon$ -greedy observes all endogenous variables whereas CBO with OSCO only observes the MOS  $\mathbf{O}_{G,Y}^Z = \{Z, Y\}$ . That CBO uses most of the evaluation budget on intervening whereas CBO with OSCO uses most of the budget on observations can be explained by two main reasons. First, the definition of  $\epsilon$  in [2, Eq. 6] implies that the probability of observing in CBO with  $\epsilon$ -greedy is close to 0 when the number of previously collected observations is low. Second, the optimal stopping formulation in (11) implies that CBO with OSCO will observe rather than intervene when it is more cost-effective.

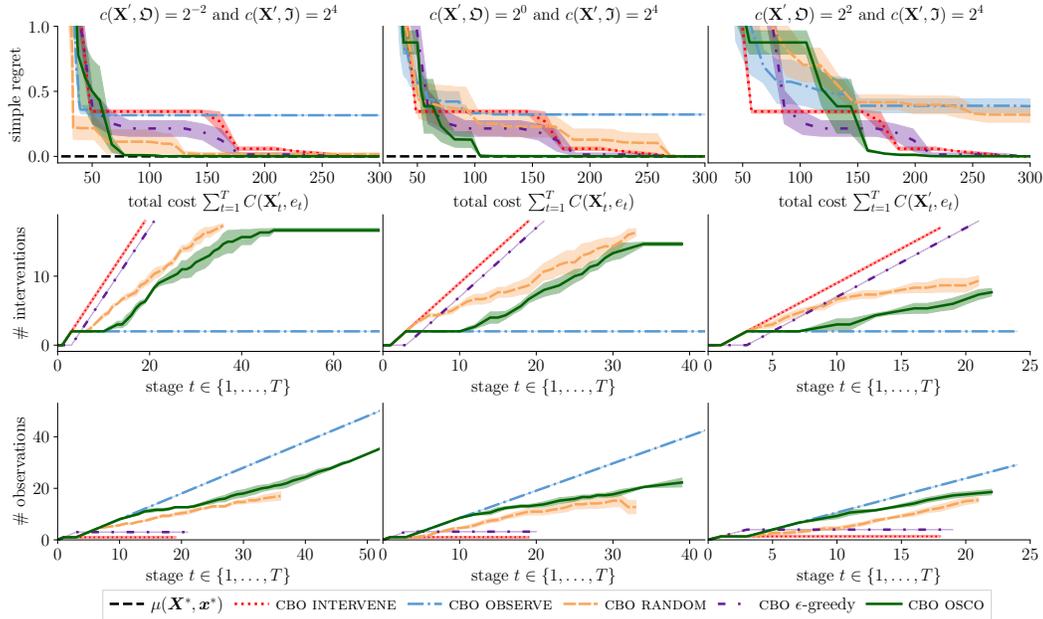


Figure 9: Convergence curves for CBO with different policies for balancing the intervention-observation trade-off when solving (3) for the chain SCM (Fig. 4a); the columns relate to evaluations with different observation costs  $c(\mathbf{X}', \mathcal{D})$ ; the top row shows the objective value against the evaluation cost; the middle and bottom rows show the number of interventions ( $e_t = \mathcal{J}$ ) and observations ( $e_t = \mathcal{D}$ ) at different stages of the optimisation; the curves indicate the mean and standard deviation ( $\pm \frac{\sigma}{\sqrt{3}}$ ) over three evaluations with different random seeds.

Figure 9 shows convergence curves of CBO with OSCO and the baselines introduced above for different observation costs  $c(\mathbf{X}, \mathcal{D})$ . We note that the OBSERVE and RANDOM baselines do not always converge to the optimum within the prescribed evaluation budget (see Appendix G for the list of hyperparameters). We further observe that CBO with OSCO on average reaches the optimum at a lower cost than all baselines.

We also compare the performance of OSCO on the chain SCM with the performance of MCBO [60]. Figure 10 shows convergence curves of MCBO with OSCO and the baselines introduced in §6 for different observation costs  $c(\mathbf{X}, \mathcal{D})$ . We note that none of the MCBO policies find the optimum. This is consistent with the findings in [60, Fig. 6] and can be explained by the design of MCBO, which is optimised for minimising the cumulative regret rather than the simple regret. We further note that the measured benefit of adding OSCO to MCBO for the chain SCM is lower than that of CBO (cf. Fig. 10). More specifically, when the observation cost is low (see e.g. the right plot in Fig. 10), MCBO with OSCO yields better results than plain MCBO. When the observation costs are high however (see e.g. the left plot in Fig. 10), MCBO with OSCO leads to slower convergence. One reason why OSCO works better with CBO than MCBO is that it can utilise MOS (Def. 4) to limit the number of observations (see §6 for details). We speculate that another reason is the different way of integrating observational data in the probabilistic models  $\hat{\mu}$  and  $\hat{\mathbf{F}}$ . In CBO, the observational data is integrated with the interventional data by using a causal prior on the interventional distributions whereas in MCBO the functions  $\hat{\mathbf{F}}$  are fitted directly based on both observational and interventional data.

## F.2 Chain SCM with an unobserved confounder

Figure 11 and Fig. 12 show convergence curves of CBO and MCBO with different policies for balancing the intervention-observation trade-off for the chain SCM with an unobserved confounder (see Fig. 4b). We observe that CBO with OSCO performs best on average and that the results resemble those obtained for the chain SCM without the unobserved confounder (see Appendix F.1). Looking at the second and third rows in the figures, we see that CBO and MCBO with OSCO focuses on collecting observations

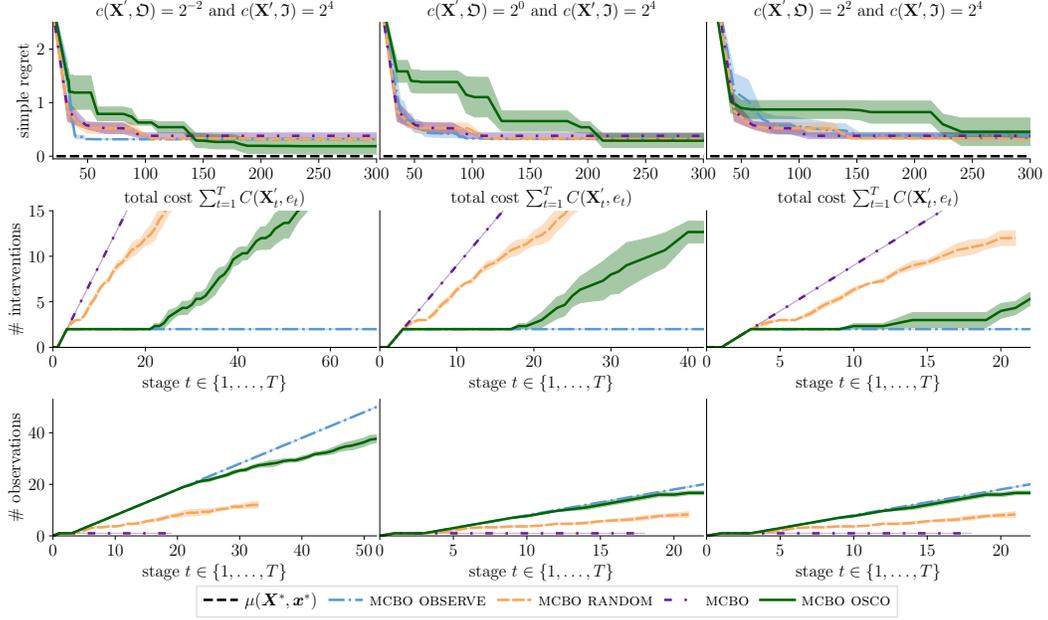


Figure 10: Convergence curves for MCBO with different policies for balancing the intervention-observation trade-off when solving (3) for the chain SCM (Fig. 5); the columns relate to evaluations with different observation costs  $c(\mathbf{X}', \mathcal{D})$ ; the top row shows the objective value against the evaluation cost; the middle and bottom rows show the number of interventions ( $e_t = \mathcal{J}$ ) and observations ( $e_t = \mathcal{D}$ ) at different stages of the optimisation; the curves indicate the mean and standard deviation ( $\pm \frac{\sigma}{\sqrt{3}}$ ) over three evaluations with different random seeds.

in the beginning of the optimisation and then successively increases the frequency of interventions. This contrasts with CBO and MCBO without OSCO, which almost exclusively intervenes.

### F.3 PSA SCM

The PSA SCM (see Fig. 4c) is based on a real healthcare setting [20] where interventions correspond to dosage prescriptions of statins and/or aspirin to control Prostate-Specific Antigen (PSA) levels, which should be minimised. This SCM is benchmarked in both [2] and [60].

Figure 13 and Fig. 14 show convergence curves of CBO and MCBO with OSCO and the baselines introduced in §6 for different observation costs  $c(\mathbf{X}, \mathcal{D})$ . We note that the only policies that consistently find the optimum are CBO, CBO with OSCO, MCBO, and MCBO with OSCO. We also note that OSCO performs, on average, better than CBO and MCBO. The differences are however relatively small. We believe that the reason why the differences are relatively small is that both CBO and MCBO finds the optimum in the chain SCM after only a couple of interventions, diminishing the need to utilise observational data. This is because the optimal intervention in the PSA SCM is at the endpoints of the domains, i.e.  $(\mathbf{X}^*, \mathbf{x}^*) = (\{\text{aspirin, statin}\}, (0, 1))$ , which is easy to find.

### F.4 Synthetic SCM

Figure 15 shows convergence curves of CBO with different policies for balancing the intervention-observation trade-off for the synthetic SCM with the causal graph in Fig. 2a. We observe that both the policy that always observes and CBO with OSCO performs best on average. This result suggests to us that the most cost-effective way to find the optimal intervention for this SCM is to collect observations and estimate the causal effects via the do-calculus.

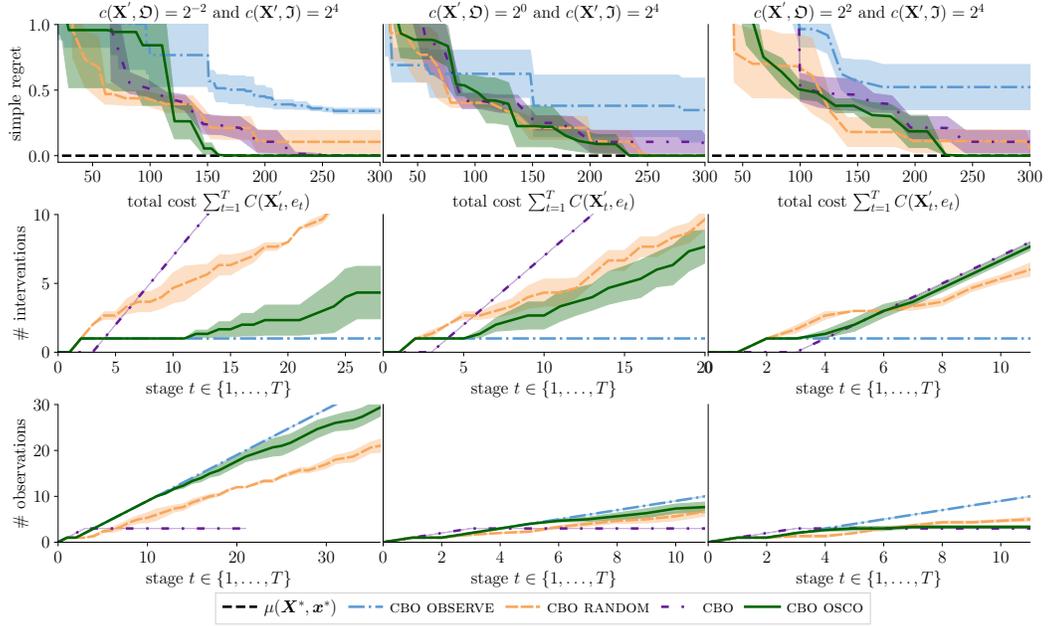


Figure 11: Convergence curves for CBO with different policies for balancing the intervention-observation trade-off when solving (3) for the chain SCM with an unobserved confounder (Fig. 1a); the columns relate to evaluations with different observation costs  $c(\mathbf{X}', \mathcal{D})$ ; the top row shows the objective value against the evaluation cost; the middle and bottom rows show the number of interventions ( $e_t = \mathcal{J}$ ) and observations ( $e_t = \mathcal{D}$ ) at different stages of the optimisation; the curves indicate the mean and standard deviation ( $\pm \frac{\sigma}{\sqrt{3}}$ ) over three evaluations with different random seeds.

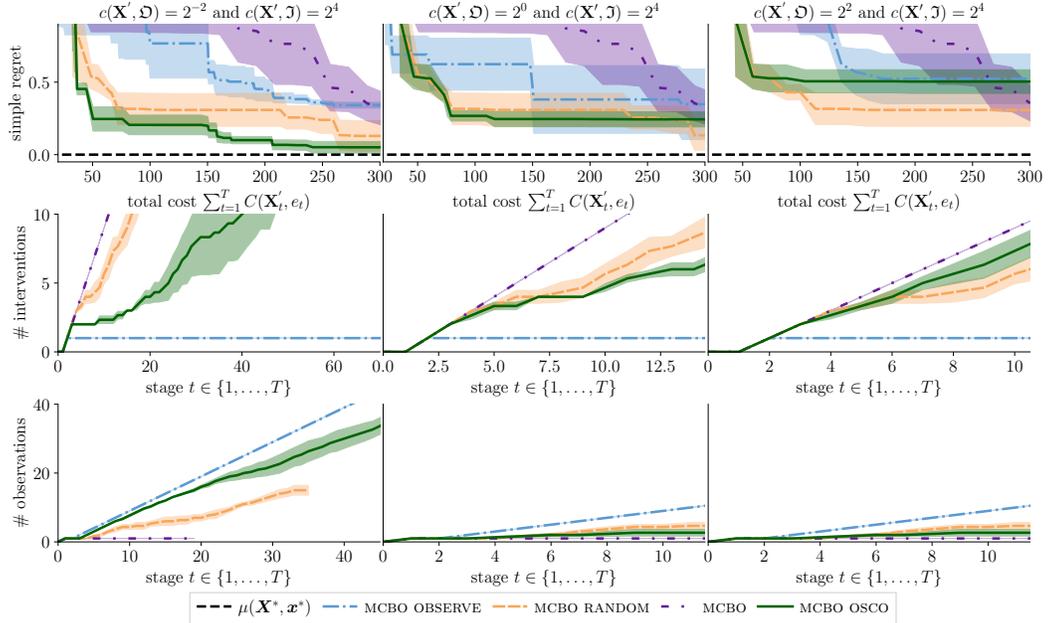


Figure 12: Convergence curves for MCBO with different policies for balancing the intervention-observation trade-off when solving (3) for the chain SCM with an unobserved confounder (Fig. 1a); the columns relate to evaluations with different observation costs  $c(\mathbf{X}', \mathcal{D})$ ; the top row shows the objective value against the evaluation cost; the middle and bottom rows show the number of interventions ( $e_t = \mathcal{J}$ ) and observations ( $e_t = \mathcal{D}$ ) at different stages of the optimisation; the curves indicate the mean and standard deviation ( $\pm \frac{\sigma}{\sqrt{3}}$ ) over three evaluations with different random seeds.

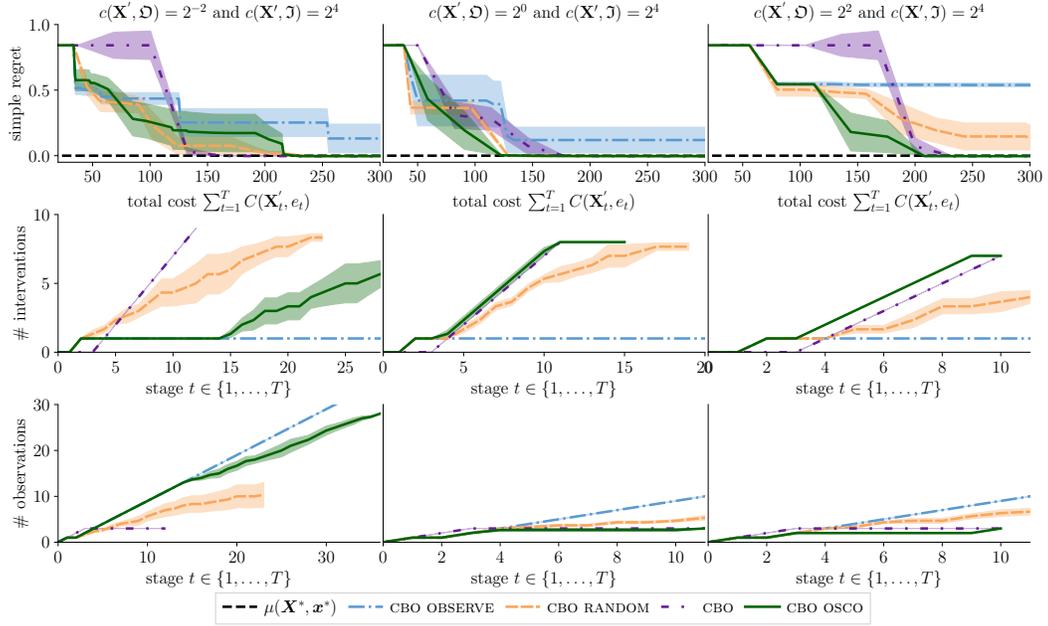


Figure 13: Convergence curves for CBO with different policies for balancing the intervention-observation trade-off when solving (3) for the PSA SCM (Fig. 4c); the columns relate to evaluations with different observation costs  $c(\mathbf{X}', \mathcal{D})$ ; the top row shows the objective value against the evaluation cost; the middle and bottom rows show the number of interventions ( $e_t = \mathcal{J}$ ) and observations ( $e_t = \mathcal{D}$ ) at different stages of the optimisation; the curves indicate the mean and standard deviation ( $\pm \frac{\sigma}{\sqrt{3}}$ ) over three evaluations with different random seeds.

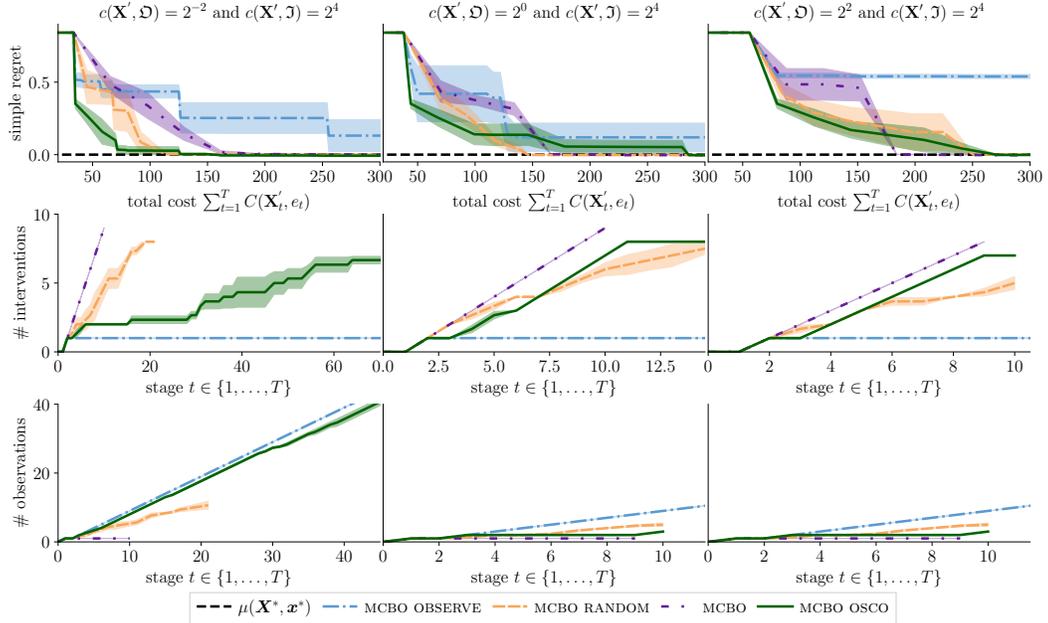


Figure 14: Convergence curves for MCBO with different policies for balancing the intervention-observation trade-off when solving (3) for the PSA SCM (Fig. 4c); the columns relate to evaluations with different observation costs  $c(\mathbf{X}', \mathcal{D})$ ; the top row shows the objective value against the evaluation cost; the middle and bottom rows show the number of interventions ( $e_t = \mathcal{J}$ ) and observations ( $e_t = \mathcal{D}$ ) at different stages of the optimisation; the curves indicate the mean and standard deviation ( $\pm \frac{\sigma}{\sqrt{3}}$ ) over three evaluations with different random seeds.

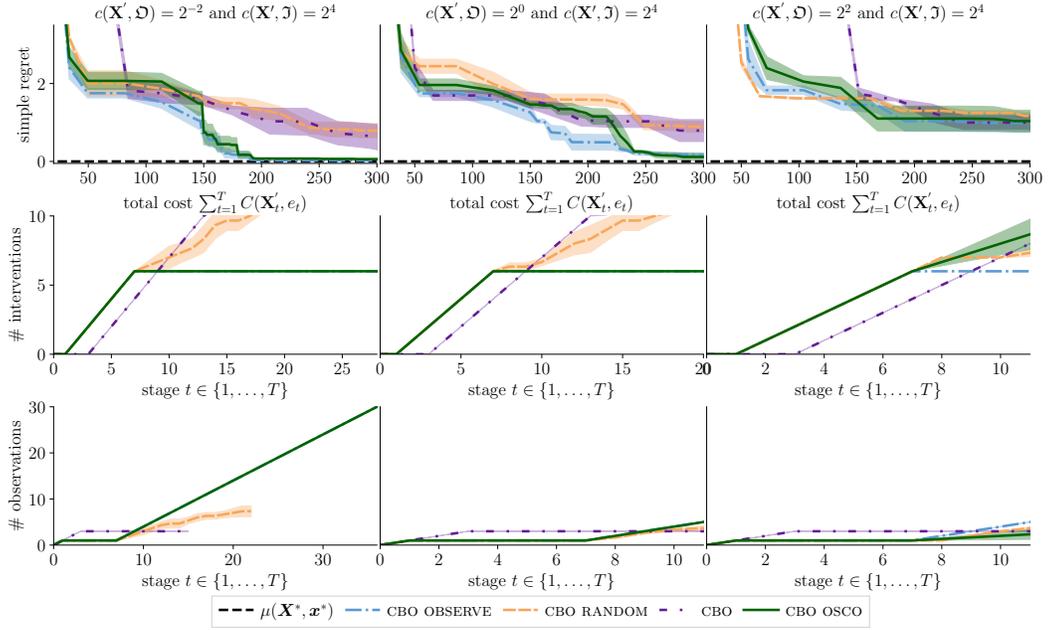
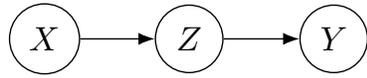


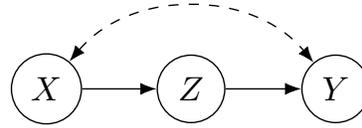
Figure 15: Convergence curves for CBO with different policies for balancing the intervention-observation trade-off when solving (3) for the synthetic SCM in Fig. 2a; the columns relate to evaluations with different observation costs  $c(\mathbf{X}', \mathcal{D})$ ; the top row shows the objective value against the evaluation cost; the middle and bottom rows show the number of interventions ( $e_t = \mathcal{J}$ ) and observations ( $e_t = \mathcal{D}$ ) at different stages of the optimisation; the curves indicate the mean and standard deviation ( $\pm \frac{\sigma}{\sqrt{3}}$ ) over three evaluations with different random seeds.

## Appendix G Hyperparameters

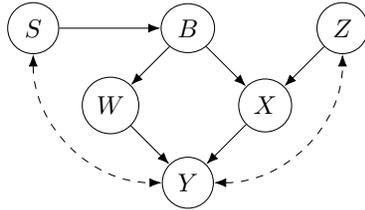
Herein we provide the hyperparameters used for all the experiments. See Fig. 16 for the relevant DAGs and their corresponding hyperparameter tables.



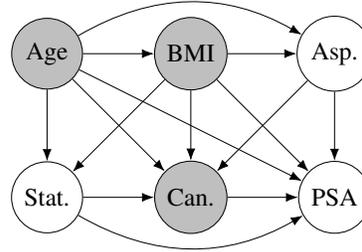
(a) Table 4.



(b) Table 4 and Appendix G.2.



(c) Table 5.



(d) Table 6.

Figure 16: DAGs used for the experimental section of this paper. Each DAG is associated with a table of experimental hyperparameters, found in the caption of each figure. The causal MAB experiment uses the DAG in sub-figure (c) with a different SCM.

## G.1 Hyperparameters for the chain SCM

Table 4: Hyperparameters for the chain SCM in Fig. 4a.

Parameter	Description	Value
$\mathbf{U}$	set of exogenous variables	$\{\epsilon_X, \epsilon_Z, \epsilon_Y\}$
$\mathbf{V}$	set of endogenous variables	$\{X, Y, Z\}$
$\mathbf{X}$	set of manipulative variables	$\{X, Z\}$
$\mathbf{Y}$	set of target variables	$\{Y\}$
$\mathbf{N}$	set of non-manipulative variables	$\{Y\}$
$\mathbf{F}$	set of functions in the SCM	$\{f_X, f_Z, f_Y\}$
$\text{dom}(X)$	domain of the random variable $X$	$[-5, 5] \subset \mathbb{R}$
$\text{dom}(Z)$	domain of the random variable $Z$	$[-5, 20] \subset \mathbb{R}$
$\text{dom}(Y)$	domain of the random variable $Y$	$[-5, 5] \subset \mathbb{R}$
$f_X$	function in the SCM	$f_X: X = \epsilon_X$
$f_Z$	function in the SCM	$f_Z: Z = e^{-X} + \epsilon_Z$
$f_Y$	function in the SCM	$f_Y: Y = \cos(Z) - e^{-\frac{Z}{20}} + \epsilon_Y$
$\epsilon_X$	Gaussian noise term in $f_X$	$\epsilon_X \sim \mathcal{N}(\mu = 0, \sigma = 1)$
$\epsilon_Z$	Gaussian noise term in $f_Z$	$\epsilon_Z \sim \mathcal{N}(\mu = 0, \sigma = 0.5)$
$\epsilon_Y$	Gaussian noise term in $f_Y$	$\epsilon_Y \sim \mathcal{N}(\mu = 0, \sigma = 0.1)$
$K$	evaluation budget in (4)	300
$\mathbf{D}_1$	initial dataset of observations and interventions	$\emptyset$
$\hat{\mu}$	probabilistic model of $\mu$ , see (3)	Gaussian process (GP)
$\hat{\mathbf{F}}$	probabilistic model of $\mathbf{F}$	GP
GP kernel	kernel for $\hat{\mu}$ and $\hat{\mathbf{F}}$	causal RBF kernel [2]
RBF length-scale	parameter for the causal RBF kernel	1
GP variance	parameter for the GP in [23]	$e^{-5}$
acquisition function	acquisition function for CBO	CEI [2]
$\eta$	weighting factor in (8)	2
$\kappa$	weighting factor in (8)	1
$\tau$	weighting factor in (8)	5
$\mathbf{M}_{\mathcal{G}, Y}^{\mathbf{V}}$	set of MISS (Def. 2)	$\{\{Z\}, \{X, Z\}\}$
$\mathbf{P}_{\mathcal{G}, Y}^{\mathbf{V}}$	set of POMISS (Def. 3)	$\{\{Z\}\}$
$\mathbf{O}_{\mathcal{G}, Y}^X$	MOS (Def. 4) for $P(Y   \text{do}(X = x))$	$\{X, Z, Y\}$
$\mathbf{O}_{\mathcal{G}, Y}^Z$	MOS (Def. 4) for $P(Y   \text{do}(Z = z))$	$\{Z, Y\}$
$c(\cdot, \mathcal{D})$	observation costs	$c(\mathbf{L}, \mathcal{D}) =  \mathbf{L} 2^{-2} \quad \forall \mathbf{L} \in \mathcal{P}(\mathbf{V})$
$c(\cdot, \mathcal{I})$	intervention costs	$c(\mathbf{L}, \mathcal{I}) =  \mathbf{L} 2^4 \quad \forall \mathbf{L} \in \mathcal{P}(\mathbf{X})$
$\gamma$	discount factor for the stopping problem	1
MCBO batch size	batch size for $\pi_{\mathcal{O}}$ in MCBO	32
MCBO $\beta$	exploration-exploitation parameter in MCBO	0.5

## G.2 Hyperparameters for the chain SCM with an unobserved confounder

The SCM in Fig. 1a uses the same hyperparameters as Fig. 4a listed in Table 4, with the differences that a) there is an unobserved confounder  $\epsilon_{XY} \sim \mathcal{N}(\mu = 0, \sigma = 1)$  in both  $f_Y$  and  $f_X$ ; b) the set of POMISS is  $\mathbf{P}_{\mathcal{G}, Y}^{\mathbf{V}} = \{\emptyset, \{Z\}\}$ ; c) the MOS for  $P(Y | \text{do}(Z = z))$  is  $\mathbf{O}_{\mathcal{G}, Y}^Z = \{X, Z, Y\}$ ; and d)  $\epsilon_Z \sim \mathcal{N}(\mu = -1, \sigma = 0.5)$ .

### G.3 Hyperparameters for the synthetic example SCM

The functions ( $\mathbf{F}$ ) for the synthetic example SCM in Fig. 2a, adapted from [2], are given by

$$\begin{aligned}
 U_{SY} &= \epsilon_{SY} && \text{(unobserved confounder between } S \text{ and } Y) \\
 U_{ZY} &= \epsilon_{ZY} && \text{(unobserved confounder between } Z \text{ and } Y) \\
 f_S: S &= U_{SY} + \epsilon_S \\
 f_B: B &= S + \epsilon_B \\
 f_Z: Z &= e^{-U_{ZY}} + \epsilon_Z \\
 f_W: W &= \frac{e^{-B}}{10} + \epsilon_W \\
 f_X: X &= \cos(Z) + \frac{B}{10} + \epsilon_X \\
 f_Y: Y &= \cos(W) + \sin(X) + U_{SY} + U_{ZY} \cdot \epsilon_Y
 \end{aligned} \tag{36}$$

Set of MISS

$$\begin{aligned}
 &\{\emptyset, \\
 &\{Z\}, \{X\}, \{W\}, \{B\}, \{S\}, \\
 &\{S, W\}, \{X, W\}, \{Z, W\}, \{B, Z\}, \{B, X\}, \{X, S\}, \{B, W\}, \{S, Z\}, \\
 &\{Z, S, W\}, \{B, Z, W\}\}.
 \end{aligned} \tag{37}$$

Set of POMISS

$$\begin{aligned}
 &\{\emptyset, \\
 &\{X\}, \{W\}, \{Z\}, \\
 &\{B, W\}, \{X, W\}, \{Z, W\}\}.
 \end{aligned} \tag{38}$$

Table 5: Hyperparameters for the synthetic SCM example in Fig. 2a.

Parameter	Description	Value
$\mathbf{U}$	set of exogenous variables	$\{\epsilon_{SY}, \epsilon_{ZY}, \epsilon, \{\epsilon_i\}_{i=S,B,Z,W,X}\}$
$\mathbf{V}$	set of endogenous variables	$\{S, B, Z, W, X, Y\}$
$\mathbf{X}$	set of manipulative variables	$\{S, B, Z, W, X\}$
$\mathbf{Y}$	set of target variables	$\{Y\}$
$\mathbf{N}$	set of non-manipulative variables	$\emptyset$
$\mathbf{F}$	set of functions in the SCM	$\{f_j\}_{j=S,B,Z,W,X,Y}$
$\text{dom}(S)$	domain of the random variable $S$	$[-5, 4] \subset \mathbb{R}$
$\text{dom}(B)$	domain of the random variable $B$	$[-5, 4] \subset \mathbb{R}$
$\text{dom}(W)$	domain of the random variable $W$	$[-5, 5] \subset \mathbb{R}$
$\text{dom}(X)$	domain of the random variable $X$	$[-6, 3] \subset \mathbb{R}$
$\text{dom}(Z)$	domain of the random variable $Z$	$[-5, 4] \subset \mathbb{R}$
$\{f_j\}_{j \in \mathbf{V}}$	functions in the SCM	see (36)
$\{\epsilon_j\}_{j \in \mathbf{V} \setminus \{W,X\}}$	Gaussian noise terms	$\epsilon_j \sim \mathcal{N}(\mu = 0, \sigma = 0.1)$
$\epsilon_W$	Gaussian noise term	$\epsilon_W \sim \mathcal{N}(\mu = 0, \sigma = 2)$
$\epsilon_X$	Gaussian noise term	$\epsilon_X \sim \mathcal{N}(\mu = 0, \sigma = 2)$
$\epsilon_{SY}$	Unobserved confounder term	$\epsilon_{SY} \sim \mathcal{N}(\mu = 0, \sigma = 0.1)$
$\epsilon_{ZY}$	Unobserved confounder term	$\epsilon_{ZY} \sim \mathcal{N}(\mu = 0, \sigma = 0.1)$
$K$	evaluation budget in (4)	300
$\mathbf{D}_1$	initial dataset of observations and interventions	$\emptyset$
$\hat{\mu}$	probabilistic model of $\mu$ , see (3)	Gaussian process (GP)
$\hat{\mathbf{F}}$	probabilistic model of $\mathbf{F}$	GP
GP kernel	kernel for $\hat{\mu}$ and $\hat{\mathbf{F}}$	causal RBF kernel [2]
RBF length-scale	parameter for the causal RBF kernel	1
GP variance	parameter for the GP in [23]	$e^{-5}$
acquisition function	acquisition function for CBO	CEI [2]
$\eta$	weighting factor in (8)	2
$\kappa$	weighting factor in (8)	1
$\tau$	weighting factor in (8)	5
$\mathbf{M}_{\mathcal{G},Y}^{\mathbf{V}}$	MISs (Def. 2)	see (37)
$\mathbf{P}_{\mathcal{G},Y}^{\mathbf{V}}$	POMISs (Def. 3)	see (38)
$\mathbf{O}_{\mathcal{G},Y}^{\emptyset}$	MOS (Def. 4)	$\mathbf{V}$
$\mathbf{O}_{\mathcal{G},Y}^X$	MOS (Def. 4)	$\{X, B, Z, Y\}$
$\mathbf{O}_{\mathcal{G},Y}^W$	MOS	$\{B, W, Y\}$
$\mathbf{O}_{\mathcal{G},Y}^Z$	MOS	$\mathbf{V}$
$\mathbf{O}_{\mathcal{G},Y}^{\{B,W\}}$	MOS	$\{B, W, S, Y\}$
$\mathbf{O}_{\mathcal{G},Y}^{\{X,W\}}$	MOS	$\{W, X, B, Z, Y\}$
$\mathbf{O}_{\mathcal{G},Y}^{\{Z,W\}}$	MOS	$\mathbf{V}$
$c(\cdot, \mathcal{D})$	observation costs	$c(\mathbf{L}, \mathcal{D}) =  \mathbf{L} 2^{-2} \quad \forall \mathbf{L} \in \mathcal{P}(\mathbf{V})$
$c(\cdot, \mathcal{J})$	intervention costs	$c(\mathbf{L}, \mathcal{J}) =  \mathbf{L} 2^4 \quad \forall \mathbf{L} \in \mathcal{P}(\mathbf{X})$
$\gamma$	discount factor for the stopping problem	1

#### G.4 Hyperparameters for the PSA SCM

The DAG in Fig. 4c describes the causal relationships between statin (node  $D$ ), aspirin (node  $C$ ) and prostate-specific antigen (PSA) level (node  $F$ ), mediated by a set of non-manipulative variables, adapted from [20]. We use the same SCM as Aglietti et al. [2, Appendix §5].

$$\begin{aligned}
 f_A \text{ (Age)}: A &= \mathcal{U}(55, 75) \\
 f_B \text{ (BMI)}: B &= \mathcal{N}(27.0 - 0.01 \cdot A, 0.7) \\
 f_C \text{ (Aspirin)}: C &= \sigma(-8.0 + 0.10 \cdot A + 0.03 \cdot B) \\
 f_D \text{ (Statin)}: D &= \sigma(-13.0 + 0.10 \cdot A + 0.20 \cdot B) \\
 f_E \text{ (Cancer)}: E &= \sigma(2.2 - 0.05 \cdot A + 0.01 \cdot B - 0.04 \cdot D + 0.02 \cdot C) \\
 f_F \text{ (PSA)}: F &= \mathcal{N}(6.8 + 0.04 \cdot A - 0.15 \cdot B - 0.60 \cdot D + 0.55 \cdot C + E, 0.4)
 \end{aligned} \tag{39}$$

In (39),  $\mathcal{U}(a, b)$  denotes the continuous uniform distribution on the interval  $[a, b]$ ,  $\mathcal{N}(\mu, \sigma^2)$  denotes the univariate Gaussian distribution with mean  $\mu$  and variance  $\sigma^2$  and  $\sigma(x)$  denotes the sigmoid function  $\frac{1}{1+e^{-x}}$ .

Table 6: Hyperparameters for the PSA level example in Fig. 4c .

Parameter	Description	Value
$\mathbf{U}$	set of exogenous variables	$\emptyset$
$\mathbf{V}$	set of endogenous variables	$\{A, B, C, D, E, F\}$
$\mathbf{X}$	set of manipulative variables	$\{D, C\}$
$\mathbf{N}$	set of non-manipulative variables	$\{A, B, E\}$
$\mathbf{Y}$	set of target variables	$\{F\}$
$\mathbf{F}$	set of functions in the SCM	$\{f_A, f_B, f_C, f_D, f_E, f_F\}$
$\text{dom}(A)$	domain of the random variable $A^\ddagger$	$[55, 75] \subset \mathbb{R}$
$\text{dom}(B)$	domain of the random variable $B^\ddagger$	$[24.1, 28.8] \subset \mathbb{R}$
$\text{dom}(C)$	domain of the random variable $C^\ddagger$	$[0, 1] \subset \mathbb{R}$
$\text{dom}(D)$	domain of the random variable $D^\ddagger$	$[0, 1] \subset \mathbb{R}$
$\text{dom}(E)$	domain of the random variable $E^\ddagger$	$[0, 1] \subset \mathbb{R}$
$\text{dom}(F)$	domain of the random variable $F^\ddagger$	$[4.36, 7.81] \subset \mathbb{R}$
$\{f_i\}_{i \in \mathbf{V}}$	function in the SCM	see (39)
$K$	evaluation budget in (4)	300
$\mathbf{D}_1$	initial dataset of observations and interventions	$\emptyset$
$\hat{\mu}$	probabilistic model for $\mu$ , see (3)	GP
$\hat{\mathbf{F}}$	probabilistic model for $\mathbf{F}$	GP
GP kernel	kernel for $\hat{\mu}$ and $\hat{\mathbf{F}}$	causal RBF kernel [2]
RBF length-scale	parameter for the causal RBF kernel	1
GP variance	parameter for the GP in [23]	$e^{-5}$
acquisition function	acquisition function for CBO	CEI [2]
$\eta$	weighting factor in (8)	2
$\kappa$	weighting factor in (8)	1
$\tau$	weighting factor in (8)	5
$\mathbf{M}_{\mathcal{G}, F}^{\mathbf{V}}$	set of MISSs (Def. 2)	$\{\emptyset, \{C\}, \{D\}, \{C, D\}\}$
$\mathbf{P}_{\mathcal{G}, F}^{\mathbf{V}}$	set of POMISSs (Def. 3)	$\{\{C, D\}\}$
$\mathbf{O}_{\mathcal{G}, Y}^{\{C, D\}}$	MOS (Def. 4) for $P(F \mid \text{do}(C = c), \text{do}(D = d))$	$\{A, B, C, D, F\}$
$c(\cdot, \mathcal{D})$	observation costs	$c(\mathbf{L}, \mathcal{D}) =  \mathbf{L} 2^{-2} \quad \forall \mathbf{L} \in \mathcal{P}(\mathbf{V})$
$c(\cdot, \mathcal{J})$	intervention costs	$c(\mathbf{L}, \mathcal{J}) =  \mathbf{L} 2^4 \quad \forall \mathbf{L} \in \mathcal{P}(\mathbf{X})$
$\gamma$	discount factor for the stopping problem	1
MCBO batch size	batch size for $\pi_{\mathcal{O}}$ in MCBO	32
MCBO $\beta$	exploration-exploitation parameter in MCBO	0.5

<sup>†</sup> The domains used in this experiment are the 25th and 75th percentiles of the measured variables, found in [20, Table 1].

<sup>‡</sup> Strictly this is a discrete variable which we have made continuous for computational reasons.

Where

$$P(F | \text{do}(C = c), \text{do}(D = d)) = \int P(F | A, B, C, D) P(A, B) \text{dadb}. \quad (40)$$

### G.5 Synthetic causal MAB

We consider the causal MAB setting in which the causal structure is provided by the SCM with DAG  $\mathcal{G}$  in Fig. 2a. The two unobserved confounders follow binary distributions governed by

$$\begin{aligned} P(U_{SY} = 1) &= 0.1 \\ P(U_{ZY} = 1) &= 0.05 \end{aligned}$$

and exogenous variables follow binary distributions governed by

$$\begin{aligned} P(U_S = 1) &= 0.45 \\ P(U_B = 1) &= 0.4 \\ P(U_Z = 1) &= 0.8 \\ P(U_W = 1) &= 0.3 \\ P(U_X = 1) &= 0.85 \end{aligned}$$

All variables are binary with domain  $\{0, 1\}$  and with  $\mathbf{F}$ :

$$\begin{aligned} f_S: S &= U_{SY} \oplus U_S \\ f_Z: Z &= 1 - U_{ZY} \oplus U_Z \\ f_B: B &= S \oplus U_B \\ f_W: W &= B \oplus U_W \\ f_X: X &= 1 - B \oplus Z \oplus U_X \\ f_Y: Y &= W \oplus X \oplus U_{SY} \oplus U_{ZY} \end{aligned} \quad (41)$$

where  $\oplus$  is the exclusive-or function. The set of POMISS, the set of MISS and the MOS for each intervention can be found in Table 5.

## Appendix H Pseudocode and implementation of OSCO

The optimal stopping problem described §4 can be integrated with existing causal optimisation algorithms to balance the *intervention-observation* trade-off. More specifically, given an optimisation policy  $\pi_{\text{O}}$  that determines which intervention to evaluate at each stage of the optimisation, the solution to the optimal stopping problem in (6) determines whether the intervention should be evaluated by intervention or observation. ( $\pi_{\text{O}}$  may for example be implemented by the CBO algorithm [2, Alg. 1] or the causal MAB algorithm in [37, Alg.1 ]) The pseudocode for integrating the optimal stopping problem with the existing algorithms is listed in Algorithm 1. The main computational complexity of the integration is the repeated solving of (11), which requires evaluating a potentially high-dimensional integral and evaluating the optimisation policy  $\pi_{\text{O}}$  several times. The integral can be evaluated efficiently using Monte-Carlo methods [51, 19] and the evaluations of  $\pi_{\text{O}}$  (which may involve optimisation of an acquisition function as is e.g. the case in CBO [2]) can be done in parallel. The average execution times per iteration when running CBO and MCBO with and without OSCO are shown in Fig. 17.

---

**Algorithm 1** Optimal stopping for Causal Optimisation (OSCO).
 

---

**Input:** Optimisation policy  $\pi_{\mathcal{O}}$  and causal graph  $\mathcal{G}$ .

**Output:** Optimised intervention  $(\mathbf{X}^*, \mathbf{x}^*)$ .

- 1: **procedure**
- 2:   Set  $\mathbf{D}_1 \triangleq \emptyset$  and initialise models  $\hat{\mu}_{\mathbf{D}_1}, \hat{\mathbf{F}}_{\mathbf{D}_1}$ .
- 3:   Compute set of POMISS  $\mathbf{P}_{\mathcal{G}, Y}^V$ .
- 4:   **for**  $t = 1, \dots, T$  **do**
- 5:     Set  $\mathbf{X}'_t, \mathbf{x}'_t \triangleq \pi_{\mathcal{O}}(\hat{\mu}_{\mathbf{D}_t}, \hat{\mathbf{F}}_{\mathbf{D}_t}, \mathbf{P}_{\mathcal{G}, Y}^V)$ .
- 6:     Compute  $\mathcal{T}^*$  using (11).
- 7:     **if**  $\mathcal{T}^* = 1$  **then**
- 8:       Intervene  $\text{do}(\mathbf{X}'_t = \mathbf{x}'_t)$  & measure  $Y$ .
- 9:       Set  $\mathbf{D}_{t+1} \triangleq \mathbf{D}_t \cup \{(\text{do}(\mathbf{X}'_t = \mathbf{x}'_t), Y)\}$ .
- 10:     **else**
- 11:       Observe  $\mathbf{o}_t \sim P(\mathbf{O}_{\mathcal{G}, Y}^{\mathbf{X}})$ .
- 12:       Set  $\mathbf{D}_{t+1} \triangleq \mathbf{D}_t \cup \{\mathbf{o}_t\}$ .
- 13:     **end if**
- 14:     Update models  $\hat{\mu}_{\mathbf{D}_{t+1}}$  and  $\hat{\mathbf{F}}_{\mathbf{D}_{t+1}}$ .
- 15:   **end for**
- 16:   **return**

$$(\mathbf{X}^*, \mathbf{x}^*) \in \arg \min_{\substack{\mathbf{X}' \in \mathbf{P}_{\mathcal{G}, Y}^V; \\ \mathbf{x}' \in \text{dom}(\mathbf{X}')}} \hat{\mu}(\mathbf{X}', \mathbf{x}')$$

17: **end procedure**

---

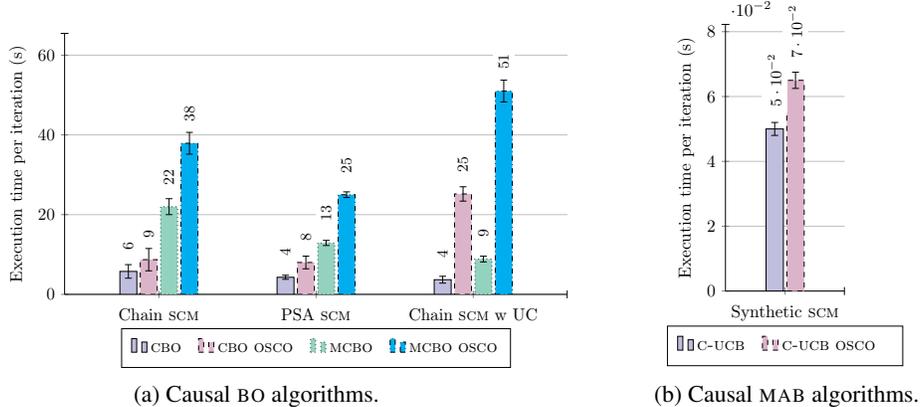


Figure 17: Execution times per iteration when running CBO [2], MCBO [60] and C-UCB [37] with and without OSCO for the example SCMs defined in §6; the height of each bar indicates the mean execution time from 100 measurements and the error bars indicate the standard deviations.

## Appendix I Background on Markovian optimal stopping problems

This appendix provides a self-contained background on MDPs and Markovian optimal stopping problems. It provides sufficient prerequisite knowledge for a reader that is not familiar with optimal stopping to follow §4 in the main body of the paper.

## I.1 Markov decision processes

A Markov Decision Process (MDP) models the control of a discrete-time dynamical system that evolves in time-steps from  $t = 1$  to  $t = T$  and is defined by the seven-tuple [11, 49]:

$$\mathcal{M} = \langle \mathbf{S}, \mathbf{A}, P_{\mathcal{M}}, r, \gamma, \rho_1, T \rangle \quad (42)$$

$\mathbf{S} \subseteq \mathbb{R}^n$  denotes the set of states,  $\mathbf{A} \subseteq \mathbb{R}^m$  denotes the set of actions,  $\gamma \in [0, 1]$  is a discount factor,  $\rho_1 : \mathbf{S} \rightarrow [0, 1]$  is the initial state distribution and  $T$  is the time horizon.  $P_{\mathcal{M}}(\mathbf{S}_{t+1} = \mathbf{s}_{t+1} \mid \mathbf{S}_t = \mathbf{s}_t, \mathbf{A}_t = \mathbf{a}_t)$  refers to the probability of transitioning from state  $\mathbf{s}_t$  to state  $\mathbf{s}_{t+1}$  when taking action  $\mathbf{a}_t$  and satisfies the Markov property  $P_{\mathcal{M}}(\mathbf{S}_{t+1} = \mathbf{s}_{t+1} \mid \mathbf{S}_t = \mathbf{s}_t) = P_{\mathcal{M}}(\mathbf{S}_{t+1} = \mathbf{s}_{t+1} \mid \mathbf{S}_1 = \mathbf{s}_1, \dots, \mathbf{S}_t = \mathbf{s}_t)$ , where  $\mathbf{s}_t \in \mathbf{S}$  and  $\mathbf{a}_t \in \mathbf{A}$  are realisations of the random vectors  $\mathbf{S}_t$  and  $\mathbf{A}_t$ . Similarly,  $r(\mathbf{s}_t, \mathbf{a}_t) \in \mathbb{R}$  is the reward when taking action  $\mathbf{a}_t$  in state  $\mathbf{s}_t$ , which we assume is bounded, i.e.  $|r(\mathbf{s}_t, \mathbf{a}_t)| \leq M < \infty$  for some  $M \in \mathbb{R}$ . If  $P_{\mathcal{M}}$  and  $r(\mathbf{s}_t, \mathbf{a}_t)$  are independent of the time-step  $t$ , the MDP is said to be *stationary* and if  $\mathbf{S}$  and  $\mathbf{A}$  are finite, the MDP is said to be *finite*.

A policy is a function  $\pi : \{1, \dots, T\} \times \mathbf{S} \rightarrow \Delta(\mathbf{A})$ . If a policy is independent of the time-step  $t$  given the current state, it is called *stationary*. An optimal policy  $\pi^*$  maximizes the expected discounted cumulative reward over the time horizon:

$$\pi^* \in \operatorname{argmax}_{\pi \in \Pi} \mathbb{E}_{\pi} \left[ \sum_{t=1}^T \gamma^{t-1} R_t \right] \quad (43)$$

where  $\Pi$  is the policy space,  $R_t \in \mathbb{R}$  is a random variable representing the reward at time  $t$  and  $\mathbb{E}_{\pi}$  denotes the expectation of the random vectors and variables  $(\mathbf{S}_t, R_t, \mathbf{A}_t)_{t=1, \dots, T}$  under policy  $\pi$ .

Optimal deterministic policies exist for a finite MDP with bounded rewards and either  $T < \infty$  or  $\gamma \in [0, 1)$  [49, Prop. 4.4.3 & Thm. 6.2.10]. If the MDP is also stationary and the horizon is either random or infinite with  $\gamma \in [0, 1)$ , an optimal stationary policy exists [49, Thm. 6.2.10].

The Bellman equations relate any optimal policy  $\pi^*$  to the two value functions  $V^* : \mathbf{S} \rightarrow \mathbb{R}$  and  $Q^* : \mathbf{S} \times \mathbf{A} \rightarrow \mathbb{R}$  [12]:

$$V^*(\mathbf{s}_t) = \max_{\mathbf{a}_t \in \mathbf{A}} \mathbb{E}_{\mathbf{S}_{t+1}} [R_{t+1} + \gamma V^*(\mathbf{S}_{t+1}) \mid \mathbf{S}_t = \mathbf{s}_t, \mathbf{A}_t = \mathbf{a}_t] \quad (44)$$

$$Q^*(\mathbf{s}_t, \mathbf{a}_t) = \mathbb{E}_{\mathbf{S}_{t+1}} [R_{t+1} + \gamma V^*(\mathbf{S}_{t+1}) \mid \mathbf{S}_t = \mathbf{s}_t, \mathbf{A}_t = \mathbf{a}_t] \quad (45)$$

$$\pi^*(\mathbf{s}_t) \in \operatorname{argmax}_{\mathbf{a}_t \in \mathbf{A}} Q^*(\mathbf{s}_t, \mathbf{a}_t) \quad (46)$$

where  $V^*(\mathbf{s}_t)$  and  $Q^*(\mathbf{s}_t, \mathbf{a}_t)$  denote the expected cumulative discounted reward under  $\pi^*$  for each state and state-action pair, respectively. Solving (44) – (45) means computing the value functions from which an optimal policy can be obtained via (46).

## I.2 Markovian optimal stopping problems

Optimal stopping is a classical problem domain with a well-developed theory [66, 54, 47, 16, 13, 10, 49, 24]. Many variants of the optimal stopping problem have been studied. For example, discrete-time and continuous-time problems, stationary and non-stationary problems and Markovian and non-Markovian problems. As a consequence, different solution methods for these variants have been developed. The most commonly used methods are the *martingale approach* [47, 16, 58] and the *Markovian approach* [54, 13, 49, 50, 10].

In this paper, we focus on a stationary optimal stopping problem with a finite time horizon  $T$ , discrete-time progression, a continuous state space  $\mathbf{S} \subset \mathbb{R}^n$ , bounded rewards and the Markov property. We use the Markovian solution approach and model the problem as a stationary MDP  $\mathcal{M}$ , where the system state evolves as a discrete-time Markov process  $(\mathbf{S}_t)_{t=1}^T$ . Here  $\mathbf{S}_t \in \mathbf{S}$  and  $\mathbf{s}_t$  denotes the realization of  $\mathbf{S}_t$ . At each time-step  $t$  of this process, two actions are available: “stop” (S) and “continue” (C) i.e.  $(A_t \in \{S, C\})_{t=1, \dots, T}$ . The *stop* action yields a reward  $r(\mathbf{s}_t, S)$  and terminates the process. In contrast, the *continue* action causes the process to transition to the next state according to the transition probabilities  $P_{\mathcal{M}}$  and yields the reward  $r(\mathbf{s}_t, C)$ .

A *stopping time* is a positive random variable  $1 \leq \mathcal{T} \leq T$  that is dependent on  $s_1, \dots, s_{\mathcal{T}}$  and independent of  $s_{\mathcal{T}+1}, \dots, s_T$  [47]:

$$\mathcal{T} = \inf\{t : t \geq 1, a_t = S\}, \quad (47)$$

The objective is to find a deterministic and stationary stopping policy  $\pi^* : \mathbf{S} \rightarrow \{\mathbf{S}, \mathbf{C}\}$  that maximizes the expected discounted cumulative reward of the induced stopping time  $\mathcal{T}$ :

$$\pi^* \in \operatorname{argmax}_{\pi \in \Pi} \mathbb{E}_{\pi} \left\{ \sum_{t=1}^{\mathcal{T}-1} \gamma^{t-1} r(\mathbf{S}_t, \mathbf{C}) + r(\mathbf{S}_{\mathcal{T}}, \mathbf{S}) \right\} \quad (48)$$

Due to the Markov property, any policy that satisfies (48) also satisfies the following Bellman equation:

$$\pi^*(\mathbf{s}) \in \operatorname{argmax}_{\{\mathbf{S}, \mathbf{C}\}} \left\{ \underbrace{r(\mathbf{s}, \mathbf{S})}_{\text{stop (S)}}, \underbrace{\mathbb{E}_{\mathbf{S}'} [r(\mathbf{s}, \mathbf{C}) + \gamma V^*(\mathbf{S}')] ]}_{\text{continue (C)}} \right\} \quad (49)$$

where  $V^*$  is defined in (44).